2015

A methodology to analyze surface recombination velocity and other properties of Cadmium Telluride using time resolved photoluminescence

Brady A. Johnson
University of Toledo

A Thesis

entitled

A Methodology to Analyze Surface Recombination Velocity and Other Properties of Cadmium Telluride Using Time Resolved Photoluminescence

by

Brady A. Johnson

Submitted to the Graduate Faculty as partial fulfillment of the requirements for the

Master of Science Degree in

Electrical Engineering

_____

Dr. Daniel Georgiev, Committee Chair

_____

Dr. Jung Kim, Committee Member

_____

Dr. Vijaya Devabhaktuni, Committee Member

_____

Dr. Patricia R. Komuniecki, Dean
College of Graduate Studies

The University of Toledo
December 2015

An Abstract of

A Methodology to Analyze Surface Recombination Velocity and Other Properties of Cadmium Telluride Using Time Resolved Photoluminescence

by

Brady A. Johnson

Submitted to the Graduate Faculty as partial fulfillment of the requirements for the Master of Science Degree in Electrical Engineering

The University of Toledo
September 2015

The ability to develop a methodology to extract low level parameters such as surface and bulk recombination velocities can lead to the improvements in single and polycrystalline Cadmium Telluride (CdTe) solar cell performance. Given the importance of CdTe solar cells being a competitive photovoltaic material, the ability to quickly determine such low level parameters plays a key role in enabling further improvements of the conversion efficiency. CdTe has shown its advantages of offering a low cost solution at large manufacturing scales while still displaying comparable or better efficiencies to multi-crystalline silicon that dominates today's market. The work presented here can have a direct industrial and economic impact in further enhancing those advantages.

This study focuses on extracting surface recombination velocities (S_f) along with bulk recombination velocities (S_b), minority carrier lifetimes (τ) and mobility. The approach is based on a non-contact and non-destructive Time-Resolved Photoluminscence (TRPL) spectroscopy. Our methodology consists of solving for the carrier concentration using the time dependent continuity equation, two boundary

conditions, the initial condition and an error minimization procedure to obtain those low level parameters.

This Matlab analysis software proved to be a useful addition to the standard TRPL software package. After a measurement is acquired, then analyzed by this software, a new more in-depth look at the materials quality is brought to light by extracting these parameters. The analysis method provided a novel way of constantly extracting these semiconductor properties.

I dedicate this work to my wife Kelsey Johnson, for her continued support throughout my graduate work. I also dedicate this work to my parents who have always reinforced me throughout my learning career and pushed me to never settle. I also dedicate this work to my sister for providing backing and encouragement throughout my college career. Thank you to all who have impacted my life.

Acknowledgements

I would like to acknowledge the generous support from my advisor Dr. Daniel Georgiev from the University of Toledo. Dr. Igor Sankin from First Solar for his commitment and endless hours of teaching and insight. First Solar for providing me single crystal CdTe samples along with the TRPL equipment to take the necessary measurements. Physics department at The University of Toledo for supplying me a thin film polycrystalline CdTe sample for this study. I also thank the Electrical Engineering and Computer Science (EECS) department at The University of Toledo for enrolling me and giving me a chance to earn my master's degree. Thank you to some of my fellow colleagues, Dr. Andenet Alemu, Dr. Andrei Los, Dr Ying Yao for their support. Finally, thank you to my committee members Dr. Junghwan Kim and Dr. Vijaya Devabhaktuni.

Table of Contents

List of Tables

List of Figures

List of Abbreviations

Al……...Aluminum
$CdCl_2$..…….. Cadmium Chloride
CdS……Cadmium Sulfide
CdTe……..Cadmium Telluride
Cu …….Copper
ZnO……Zinc Oxide

AM1.5……Air Mass global spectrum
FF……..Fill Factor
Mu…….……Mobility
S_b……..…. Bulk Recombination Velocity
S_f…….. Surface Recombination Velocity
Tau……Lifetime
Voc……Voltage Open Circuit

Bkg…….Background
CBD……...Chemical Bath Deposition
Conv……..Convolution
HIL…….…...High Injection Level
IRF…….….. Instrument Response Function
LIL…….…...Low Level Injection
PDEPE…….….Partial Differential Equation Parabolic-Elliptic
PDL…….…..Pulsed Diode Laser
PL…….…….Photoluminescence
PV…….Photovoltaic
SPAD……Single Photon Avalanche Diode
TCO……..……Transparent Conductive Oxide
TCSPC……..Time-Correlated Single Photon Counting
TRPL…….Time Resolved Photoluminescence

List of Symbols

Å.....Angstroms
μ .....Mobility of holes
τ.....Recombination Lifetime
∇.....Upsilon

x.....Distance
q.....Charge
T .....Temperature (Kelvin)
K.....Kelvin
t .....Time
k.....Boltzmann constant
E_v.....Valence band
E_c.....Conduction band
E_g.....Band gap
nm .....Nanometers

Chapter 1

Introduction:

1.1 Thesis Rationale

Polycrystalline thin-film cadmium telluride (CdTe) has become a dominant player in utility scale solar power plants due to its superior properties such as better temperature coefficient, low production cost, and vastly improved efficiencies. Additional improvement of CdTe solar cell performance will translate directly into further cost effectiveness of this technology. Thus, enhancement of device performance is very critical in keeping CdTe at the forefront of the photovoltaic (PV) industry. One of the avenues to improve such devices is to reduce recombination losses. The surface/interface passivation of CdTe is a very important step in reducing defect related recombination centers and ultimately improving device performance. Thus, the accurate extraction of recombination parameters after any processing step is a very critical tool in gauging the quality of the material and devices which in turn enables the optimization and fine tuning of those process steps.

1.2 Thesis Objective

In this thesis, there will be four major sub-parameters of CdTe that will be extracted from the raw data. Sub-parameters are not the usual six pack parameters that would be extracted from current versus voltage curves i.e., (efficiency, voltage open circuit, and current short circuit) but the ones that play a more fundamental role in determining those. The main goal of this thesis is to accurately extract surface recombination velocity (S_f), bulk recombination velocity (S_b), mobility (μ), and carrier lifetime (τ) of the CdTe material. Being able to extract the surface recombination is the most important and allows us to monitor and optimize fabrication process steps. If the process can be measured quickly and the loss of the minority carriers can be mitigated through process changes then the lifetime of the material can be increased leading to better device performance. Lifetime of the charge carrier is dependent upon the materials quality and composition. The S_f, S_b, and μ will directly impact the performance of the device through their influence on minority carrier lifetime. Their knowledge can also inform us on the need for improvement of any passivation layer.

1.3 Thesis Experimental flow

In order to extract and model these parameters a contactless measurement process called time-resolved photoluminescence (TRPL) technique can be used on direct bandgap photovoltaic material such as CdTe. TRPL is a precise measurement conducted by a pulsed laser source into the photovoltaic material and measuring the decay in

photoluminescence (PL) as a function of time [1]. The setup uses a single photon counting detector that will collect each photon given off by the material based upon the repetition frequency of the laser. At a certain pulse width each photon is collected and stored in an array. Later this array will be analyzed by the modeling software after the decay of the signal is finished. Meaning the material has completed the radiative recombination process and is no longer emitting photons. Thus the PL decay is incorporated inside the measurement over time. For this experiment the CdTe is measured in high injection levels (HIL). High injection levels occur when the injected laser pulse is strong enough that it will not only alter the total amount of the minority carrier concentration but also saturates the majority carrier concentration inside CdTe.

The key to the success of this thesis is the Matlab modeling software that can take the raw curves that are generated from the TRPL measurement and extract both the S_f and S_b recombination rates along with the μ and τ. Before starting any modeling of sample data the instrument response function (IRF) was taken prior to sample measurement. The reasoning behind the IRF is explained later in chapter 5 experimental setup. The modeling software uses multiple functions that pulls form Matlab's built-in library such as the parabolic-elliptic partial differential equation (PDEPE) and convolution (Conv) functions. The modeling software was broken in a few major steps that first solved for the continuity equation with initial and boundary conditions. This would solve for the carrier concentration. Next the software would calculate the PL intensity as a function of time, convolute it with the measured IRF and add in background noise. This gives the calculated PL that will be used in the next step. After subtracting the calculated PL from the actual sample decay the fitting software would calculate the

error between the two curves. Once the error was calculated the software would start to minimize the difference by adjusting the four input parameters S_f, S_b, μ, and τ. These parameters are automatically varied inside the code until the calculated decay would match the sample decay. After this fitting procedure the final parameter values are retrieved and the solution for sample is recorded.

1.4 Thesis contribution

The major contribution and final product of this work is analysis software that extracts S_f, S_b, μ, and τ after each TRPL measurement on any CdTe technology. Providing quick feedback to users as they start to vary the processes steps applied to the material. In addition, this analysis aids in a more cost effective way to monitor the crystalline quality during the fabrication of actual working devices without causing any damage or stress to the samples.

1.5 Organization of work

This work is organized in 7 chapters, the first chapter consisting of the current introduction. Chapter 2 is the general background information about the material and measuring technique. Chapters 3 and 4 are the device layout and experimental setup in order to get the raw TRPL curves. Chapter 5 is the analysis software along with the algorithms that calculated the fits. Chapters 6 and 7 present the results from the analysis software and conclusions.

Chapter 2

Background:

2.1 Cadmium Telluride Specifications

Cadmium Telluride (CdTe) belongs to the II-VI group of semiconductors. Cadmium belongs to group II and Tellurium belongs to group VI. CdTe is a cubic zinc blende crystal that generally is grown in the form of (111) plane to its substrate [2]. The CdTe in this study used samples that are in polycrystalline and single-crystal formation and are p-type. These two different types of CdTe have a direct bandgap of around 1.37-1.54 with most recordings of 1.44 eV at 300 K [3].

The p-type CdTe is considered to have a high absorbing coefficient greater than $5x10^5$ (cm^{-1}) and it persists over a wide range of wavelengths spanning from ultraviolet to the band gap of CdTe around 830nm. Short wavelength photons with energy greater than the band gap of CdTe are absorbed at the CdTe's surface. The high absorbing coefficient makes CdTe an ideal absorber. The suns air mass (AM1.5) photons that are greater than the band gap of CdTe have a 99% chance of being absorbed within 2μm of the films thickness. The AM1.5 describes a standard terrestrial solar spectral irradiance that is used globally and has a power rating of 1 kW/m^2 [4]. Measuring the device performance

using an AM1.5 reference spectrum will keep the testing impartial no matter what time of day and where in the world it is being measured. The p-CdTe majority carriers are the holes and minority carriers are the electrons. This will become more relevant later in this chapter when describing the theory behind HIL.

2.2 CdS / ZnO Specifications

The general practice to create a heterojunction with CdTe by adding cadmium sulfide (CdS) layer. The CdS is a group II-VI compound semiconductor with a direct band gap of 2.42eV. Since CdS has a wide band gap it is considered to be the "window layer" to the CdTe. It will allow most of the light to past right through it except near the UV range or its bandgap. The cell's performance can be affected due to the carrier recombination at the junction of the CdS/CdTe interface instead of inside the depletion region where the generated carriers can be collected. The thickness of the CdS layer can affect the short circuit current, the thinner it is the more current can be measured. As the CdS layer thins out it severely reduces the devices open circuit voltage and fill factor which directly affects the efficiency of the overall cell. The polycrystalline sample in this study used this CdS/CdTe stack.

We used zinc oxide (ZnO) as our passivation layer instead of the CdS layer on the single-crystal CdTe samples. Polycrystalline ZnO is widely used in various applications such as varistors and transparent conductive oxide (TCO) [5]. Here the ZnO is used because of its wide direct band gap at 3.3eV [6]. ZnO also belongs to the II-VI

semiconductor group making it an ideal candidate to grow directly on the CdTe because of lattice matching.

2.3 CdTe Solar Cell Fabrication Details

The basic CdTe solar structure makeup is as follows in the figure below.

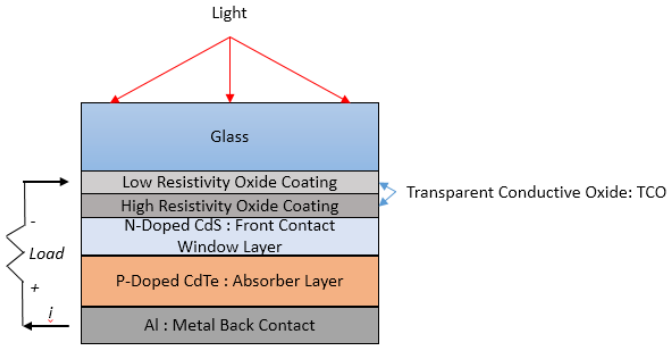

Figure 2-1: Standard format for a CdTe Solar Cell

The light will pass through side known as the “sunny side” or the glass first. Then will enter inside the transparent conducting oxide (TCO) layer. The TCO is sputtered on one side of glass substrate. This conductive layer provides the current collection from the front of the device [7]. This TCO layer provides lower absorptivity and lower resistivity but an increase in carrier mobility thus allowing increased photocurrent and decreased series resistance [7]. From there the front contact layer is formed by adding n-type Cadmium Sulfide (CdS). CdS is generally applied by chemical-bath deposition (CBD) method or Vapor transport deposition (VTD). This layer is also called the window layer because of the light it allows to pass through it instead of absorbing it due to its wide

bandgap. I will go into detail a little later in this chapter about this layer. The next layer is the absorber layer or the p-type CdTe. After the CdTe layer is deposited then a little known but heavily studied cadmium chloride ($CdCl_2$) treatment is applied and is baked in by high temperature annealing. $CdCl_2$ can be deposited by dipping into a solution, spraying or a vapor treatment. There is a significant performance boost by adding in a $CdCl_2$ anneal process around 350 - 450 degrees Celsius after it is been applied [8]. The Cl can diffuse like an atom into the CdS layer as a dopant. An increase in Voc and FF will be seen, affecting the cells overall efficiency. The improvements include the elimination of fast-recombination centers in the CdTe film, reduction of recombination centers in the junction and the elimination of small grains at the grain boundaries [9] . The benefit of adding the optimal amount of $CdCl_2$ to CdTe is having the highest cell efficiency. It is a fine line, however, of optimizing the variables of time and temperature duration and concentration of $CdCl_2$. The fabrication of CdTe solar cells depends heavily on of the last steps in fabrication process and that's the addition of copper (Cu). Copper can be deposited by spinning, spraying and chemical bath deposited (CBD). If too much copper is added, the depletion width will narrow and a lower open circuit voltage (Voc) and fill factor (FF) will persist [10]. If not enough copper is added, its full potential on the capacitance of the diode is not utilized. Finding the correct amount of copper will enhance the capacitance of the diode and will not alter the diode when under stress. The whole density will go up giving the diode a higher Voc [10]. Finally, the addition of Cu to the CdTe will aid in lowering the barrier height between the CdTe and the metal layer [11]. The last step is where the metal layer such as aluminum (Al) or Molybdenum

Nitride (MoN) is sputtered on last to seal the CdTe and connect the back contact to the front contact.

2.4 Photoluminescence

Direct band gap materials such as CdTe can emit photons when an outside source of excitation light greater than the band gap is applied to the material. Once the injected light is absorbed inside the material, electrons and holes are generated inside the conduction band (CB) and valance band (VB) respectively. Due to the Law of Mass Action, the CdTe will want to come to an equilibrium state, which starts the process of recombination of the electron hole pairs. One type of recombination is called radiative or direct band recombination. Radiative recombination describes the electron in the conduction band wanting to stabilize in a lower energy state back inside the VB removing a hole. During this process of recombination the loss of energy is given up by way of an emitted photon. This recombination process is shown in the Figure 2-2 below and will be explained in more detail in section 2.8.

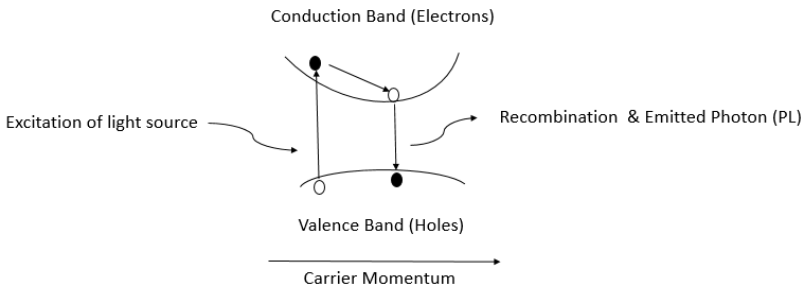

Figure 2-2: Photo induced recombination.

This methodology of collecting the emitted photons from the recombination process of absorbing the excitation light is called photoluminescence (PL) spectroscopy. PL spectroscopy has been used throughout the solar industry in order to provide a reliable characterization method to determine the crystalline quality of semiconductors. PL at low temperatures is normally taken but, room-temperature PL also provides useful information and is a popular method used. Room-temperature PL measurements lead to the better understanding of the band-edge emission and deep defect-related emissions [12]. The PL produces a single broad curve with a peak between 1.505 and 1.515 eV or about 865 nm near the bandgap of the CdTe [13]. The curve could have a full width half max (FWHM) of about 0.32 meV [12]. Generally, the amplitude of the signal is in arbitrary units, where the quality is based upon the intensity level measured. The peak of the curve will be centered on the bandgap of the material once it is in a quasi-steady state. The photon energy measured is described by the following equation [12].

$$PL = E_g + \frac{kT}{2} \tag{2.1}$$

Where E_g is the bandgap of the material, k is Boltzmann constant and T is the temperature at 300 K. Also, if any bandgap engineering is happening, the peak of the curve will shift in either direction away from the original bandgap value. The PL intensity is proportional to the rate of the recombination at the surface of the CdTe. If there are any traps or defects inside the material these could lead to recombination centers not emitting photons, causing a weak signal to be collected. The width of the curve is based upon the injection density of the excitation source. There can be measurements taken in both high and low injection levels. High injection (HIL) levels causes the

minority carrier concentration to be far above equilibrium. Low injection levels (LIL), the minority carrier concentration is just above equilibrium. These two concepts will be described in more detail in section 2.7 of this chapter. The PL can be further studied by using the time-resolved photoluminescence methodology, which is explained next.

2.5 Time-Resolved Photoluminescence

Time-resolved photoluminescence (TRPL) precisely measures the radiative PL decay as a function of time. The TRPL signal is produced by the excitation of the pulsed laser into the CdTe. The detector collects the emitted photon from the CdTe and determines the time duration it took. Typical lifetimes can be an order of picoseconds to microseconds, depending on the quality of the material. The measurement will tend to show higher lifetimes for higher quality crystals.

The system is similar to the PL, where it also depends on the wavelength of the laser to excite specific emissive states. After the carriers are generated by a short laser pulse, the junction of the CdTe to the passivation layer will then redistribute the free carriers. The rate at which the junction redistributes the carriers is dependent on recombination rate, mobility, and other junction properties [14]. The excess carrier density will decay exponentially with lifetime (τ) which is considered to be complete lifetime, with all recombination mechanisms accounted for [15]. The 641 nm excitation laser has an absorption depth of less than 0.3 μm inside the CdTe keeping it near the surface [16]. The laser is pulsed at a high repetition rate which can be upwards of 80

MHz. This repetition frequency is determined by the hardware settings and will be discussed further in the experiment setup chapter 4.

The laser pulse and the emitted photon both have times related to them. The measurement resolution time is normally hindered by the responsivity of the detector. The detectors can either be single photon collecting detectors, such as Single Photon Avalanche Diodes (SPAD) or a Photo Multiplier Tube (PMT). SPAD detectors are useful because of their speed and resolution and were used in this study. SPAD detectors can have resolutions of less than 50 ps full width half max and have detection efficiency up to 49% [17]. It is key to have a fast detector because this produces the IRF of the instrument, which is convoluted from the sample signal. Also, the narrower the IRF peak the more accurate the measurement will be and will not dominate the true signal from sample. This detector must also be fast due to dead time. Dead time correlates to the time when the photon is collected then registered and the next laser pulse is sent. If there are more than one photons being emitted after the pulse, the detector would only pick up the first photon and not count the second one. This counting would lead to an over-representation of the number of photons collected and is referred to as pile up effect on the detector [17]. The ideal cycle time needs to have only one laser pulse, one photon generated, and that photon to be collected in each cycle.

After the detector time is correlated the single photon collection module will collect each captured photon from the detector and will store them until the scan is complete [17]. The measurement is repeated at the speed of the repetition frequency. So up to 250,000 times a second. From there, the actual TRPL signal can be seen inside a histogram of the collected data.

TRPL measurements have been extracted for both single and polycrystalline CdTe. From the various research papers researchers found, polycrystalline CdTe / CdS interfaces could have a life-time value of 0.5-1 ns [1]. In other papers, 10 ns was seen at the polycrystalline CdTe / CdS interface. They also claimed for bare polycrystalline CdTe film they only saw several hundred picoseconds of lifetime [14]. The single-crystal CdTe sample have seen anywhere from 1 ns to 100 ns of lifetime based upon a 2 photon TRPL system and carrier concentration [18]. These values will vary greatly depending on the dopant, heat treatments, or chemical baths that samples may see. But these values do provide a sanity check to verify the solutions in this study seem reasonable. The exact setup and equipment used in order to collect the TRPL data for this study will be described later in chapter 4.

2.6 High Injection Level

Since the TRPL laser power density on the sample is strong enough, it will put the device under test in state known as high injection level (HIL). HIL occurs when the excess minority carrier density exceeds the doping density inside the CdTe [19]. Under HIL condition, the majority carrier density (holes in this case) will increase in order for charge neutrality to be preserved [20]. This also means that the excess electron density matches the hole density. This large amount of minority carriers leads to the material electron density (n) per unit volume approximately equaling the hole density (p) per unit volume [20]. If the material would be an n-type then this would yield the following equations which could be converted for the p-type CdTe [19].

$$n_n = n_{n0} + \delta n_n \tag{2.2}$$

$$p_n = p_{p0} + \delta p_n \tag{2.3}$$

Where n_{n0} is the thermal equilibrium and δn_n is excess carrier density and n_n is the total electron density [19]. The p_n represents the minority carrier density. While the device is in high injection levels it can be assumed that the total current is due to the diffusion current based on the drift current being so small in value. Which yields the following equation for the holes [19].

$$I_p = qA\frac{D_p \delta p_n}{L_p} = qA\frac{D_p N_d}{2L_p}\left(\sqrt{1+\frac{4n_i^2[\exp(\frac{V_a}{V_t})-1]}{n_d^2}}-1\right) \tag{2.4}$$

Where q is electronic charge, A is the area, D_p is the hole diffusion constant, L_p is the hole diffusion length, N_d is the donor doping density, V_a is the applied voltage, and V_t is thermal voltage.

The high level of injection also effects the carrier lifetime equation for band to band recombination by the following equations [11]:

$$\tau_n = \tau_p = \frac{1}{Rec*\Delta n} \tag{2.5}$$

Where Rec is the recombination and τ_p and τ_n are the hole and electron lifetimes respectively.

2.7 Low level Injection

Low level injection is induced with a source that puts the p-n junction in a forward bias but does not strain it. Low level injection is the total number of minority carriers generated are much less in concentration compared to majority carriers. This low level injection will not affect the overall majority level concentration but will affect the overall amount of minority carriers. This leads to the minority carrier recombination rates being linear [21]. This case shows where the change in hole density equals the change in electron density and is less than the hole and electron density that already existed shown by the following equations [11]:

$$\Delta n, \Delta p \ll n \; and \; p \tag{2. 6}$$

$$\tau_n = \frac{1}{R_{ec} * N_A} \tag{2. 7}$$

Where R_{ec} is the recombination and the N_A is the acceptor impurity concentration.

Unlike the HIL which is dominated by the diffusion current, LIL is dominated by the drift current in the device. The total current inside a device can be described by the following [22]:

$$J_T = J_{n(DriftCurrent)} + J_{n(DiffusionCurrent)} + J_{p(DriftCurrent)} + J_{p(DiffusionCurrent)} \tag{2.8}$$

Since the measurement taken with our device at open circuit is the sum of the hole and electron current must be equal to zero.

Taking measurements in both high and low level injections can yield detail knowledge of the depletion region and its characteristics. It will also provide valuable

information on the carrier concentration densities of the material being studied. This will help aid in further knowledge of the materials ability to generate electrons and holes. This will also assist in the understanding of the electron and hole's recombination lifetime. The material's quality can be based upon these parameters while in either high or low level injection.

2.8 Generation

The generation inside a solar cell can be the process which increases the number of free carriers available to carry charge as electron hole pairs. Carriers inside a semiconductor material can be generated by a few stimulates such as light and heat. Since TRPL uses a laser, the generation inside the CdTe will be by light. If the energy of the incoming photon is greater than the band gap (E_g) of the material the electron will become free from its bound state inside the valance band (E_v) and moves to the higher energy state inside the conduction band (E_c) [4]. These free electrons are called the free carriers and carry the charge throughout the material. The E_g is the minimum change in energy required for the electron to become excited [4]. As the energy is emitted from the photon and passed to the electron the photon ceases to exist [19]. This process of absorbing a photon and creating an electron-hole pair summarizes generation. During the generation process, the electron and hole generation rates are equal and are given by [19]:

$$G_{p,light} = G_{n,light} = \alpha \frac{P_{opt}(x)}{E_{ph} A} \tag{2.9}$$

Where α is the absorption coefficient of the semiconductor, P_{opt} optical power, x is the distance inside the material, E_{ph} is the energy of the photon and A is the area. Generally speaking the generation rate is at greatest when it is near the surface of the material. The deeper the absorption of the light inside the semiconductor the less optical power there is. This loss of the ability to create generation is described by [19]:

$$\frac{dP_{opt}(x)}{dx} = -\alpha P_{opt}(x) \tag{2.10}$$

Therefore, if one was calculating the generation rate of carriers, the optical power would also need to be calculated based upon the thickness of the material.

2.9 Recombination

Opposite to the generation process is the process known as recombination. Direct band gap materials such as CdTe can emit photons when photon energy of an excitation light greater than the band gap is applied to the material. Once the photons are absorbed inside the material electrons and holes are formed inside the conduction band (CB) and valance band (VB) equally. The driving force behind recombination is that the system will normally want to transition to equilibrium of the carrier concentration. Most likely during the recombination of the electron hole pairs there can be an emission of a photon. This process is shown in the Figure 2-3. Once the free electron relaxes by giving off its energy in way of heat or light it will stabilize back inside valance band recombining with a hole.

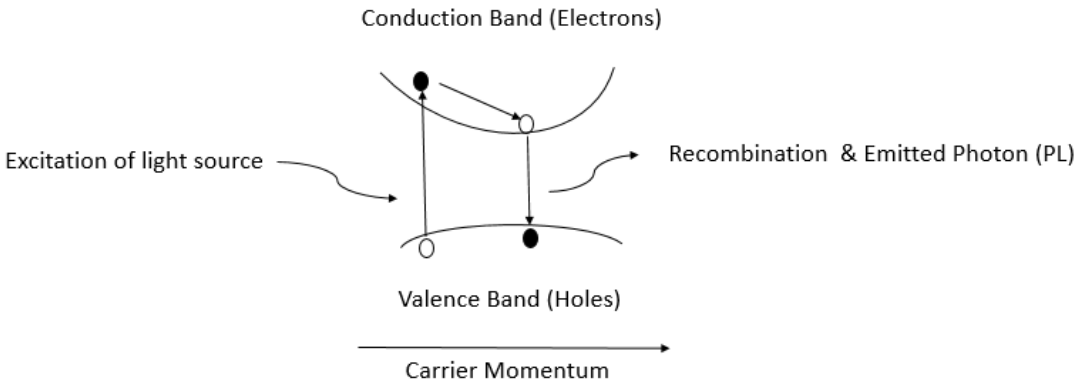

Figure 2-3: Photo induced recombination

Recombination is the detriment to the generation inside a solar cell. Meaning you want a higher generation rate than you do a recombination rate. The recombination of the electron hole pairs leads to the possibility of loss in voltage and current inside the solar cells. The recombination rate is enhanced significantly by impurities or defects found inside the crystal structure or at the surface of the material. Recombination can be described in terms of carrier concentration opposite to that of generation and is based on the following equation [11]:

$$pn > ni^2 \tag{2. 11}$$

Since CdTe is a direct band gap material its recombination mechanism is driven by band to band or radiative recombination. This band to band recombination means the electron inside the conduction band will then drop through the band gap, as its dropping it

will emit a photon as it is giving up its excess energy and will recombine with the hole in the E_v. Recombination can be described as the following equation [11]:

$$R_e = R_{ec} * pn \tag{2. 12}$$

Where R_{ec} is the recombination coefficient and is related to the thermal generation (G_{th}) by the following equation [11]:

$$R_{ec} = \frac{G_{th}}{n_i^2} \tag{2.13}$$

Or another way of showing this inside a p-type CdTe would look similar to the following [19]:

$$U_n = R_n - G_n = \frac{n_p - n_{p0}}{\tau_n} \tag{2.14}$$

Where U_n is the net recombination rate of electrons, R_n is the electron recombination rate, G_n is the generation rate, and τ_n is the electron lifetime. This type of recombination is important to understand because the surfaces and interfaces typically contain large amounts of recombination centers due to the abrupt end of the semiconductor crystal [19]. For this study we will focus on the non-radiative recombination type otherwise known as Schockley-Read-Hall (SHR) recombination. There is a possibility of a trap inside the band gap or a defect at the surface of the material that may capture the electron and the energy given off will be converted to a photon or heat [23]. This heat is considered to be non-productive inside a solar cell and needs to be minimized to maximize the efficiency of the device. The higher surface recombination is indicative of the lower lifetimes recorded.

2.10 Mobility

Carrier transport can be assimilated as the combination of the electron and hole mobility. Generally speaking, electron mobility will have higher velocity than the holes. Mobility of polycrystalline CdTe is known to be [11]: μ_n = 1,050 (cm^2 / V-s), and μ_p = 100 (cm^2 / V-s)

It was found in other papers that the mobility of polycrystalline CdTe at room temperature should be around the following: [24] μ_n = 500 (cm^2 / V-s), and μ_p = 60 (cm^2 / V-s). Mobility used by NREL in their studies for their test of polycrystalline CdTe was around 320 cm^2/V-s [25]. Single-crystal CdTe's mobility was even higher. Similar to the τ, mobility is heavily dependent on the preparation of CdTe. Mobility is affected by a few mechanisms such as heat, light, and doping. All of those factors will greatly influence the calculated mobility value.

For this study the mobility extracted will be considered ambipolar mobility. Where ambipolar transport is known as, when the excess electrons and holes do not move independently of each other, but have the same drift or diffusion with the same effective mobility or diffusion coefficient. [26]

Chapter 3

Device Structure:

3.1 Device Structure Introduction

For this study CdTe was tested in both single-crystal and polycrystalline forms. The single-crystal samples had zinc oxide (ZnO) as its passivation layer. The polycrystalline sample had CdS as its passivation layer. These two sample types will be described in more detail going forward in this chapter.

3.1 Single-Crystal CdTe

The single-crystal CdTe samples came pre-polished on both sides. Polishing helps aid in the reduction of surface dislocations and defects, and lattice strains [27]. Polishing also helps prepare the surface for another material to be deposited on top of it. There were two single crystal CdTe samples with a passivation layer made of a direct band gap of ZnO. ZnO was used since it is considered to have a wide band gap of 3.3eV. This wide band gap allows the wavelength of the laser to pass through it acting as a window

between it and the CdTe material. For this experiment the single crystal CdTe samples would have a side view shown in Figure 3.1.

Figure 3-1: Single crystal CdTe with ZNO grown on top.

The passivation layer of ZnO was sputtered to a thickness of 200Å on top of the CdTe. The single crystal CdTe layer was 8 microns thick. The junction between the CdTe and ZnO interface and the CdTe surfaces of interest. This is where the surface recombination velocities will be solved for. The two single crystal samples were provided by Fist Solar and the ZnO layer was deposited at the University of Toledo.

3.2 Polycrystalline CdTe

The polycrystalline CdTe sample provided by the University of Toledo physics department was patterned with 18 metal contact pads on a 10 cm by 10 cm glass substrate. These contact pads were actual working devices and care was taken to measure in the non-working zones. This sample's pattern looks similar to Figure 3-2 below. The aluminum metal contact pads are shaded in the light gray circle patterns. The solder line connected to the TCO is the silver outline around all cells which provides the grounding of the diodes. The dark gray filled portion inside square represents the exposed CdTe surface.

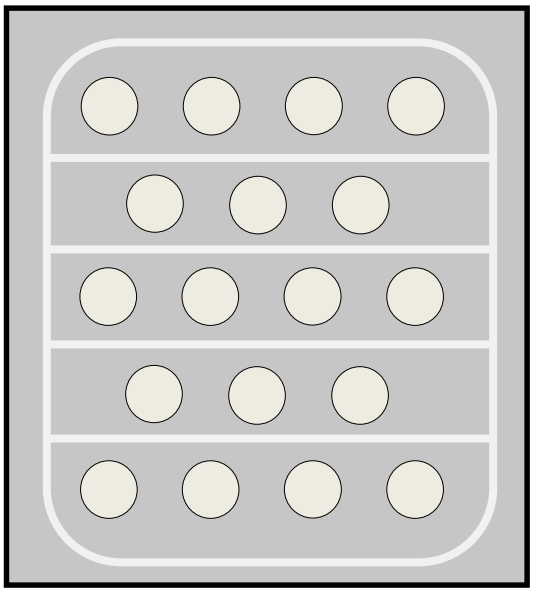

Figure 3-2: Thin-film CdTe cell sample

Unlike the single crystal stack, this sample used CdS as the window layer to the CdTe. A standard CdTe solar cell stack sequence was used as seen in Figure 3-3.

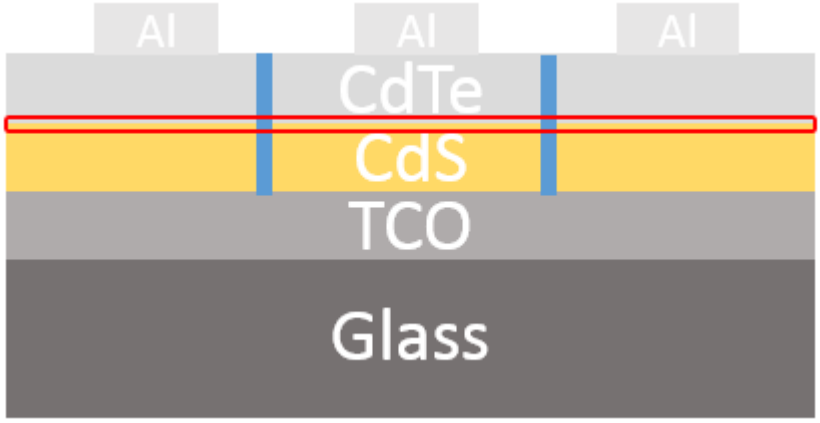

Figure 3-3: A side cut-out view of a standard CdTe solar cell showing the stack sequence

This polycrystalline sample follows the basic stack formatting that was described earlier in chapter 2. The Al contact pads provide the positive pin placements and the blue

thin rectangle boxes show where the sample would have been scraped down to the TCO then soldered to provide the grounding. However, with this study being focused on a non-contact measurement this circuitry will not be utilized. The interface between the CdTe and CdS and the exposed CdTe surface are the areas of interest for this study.

Chapter 4

Experimental Details:

4.1 Experimental Introduction / Overview

A general overview of the setup, sample prep, and experimental details will be explained, followed by a more thorough breakdown inside the sections of this chapter.

The first aspect of the project is the hardware components and settings used to acquire measurements. TRPL instrument components developed by PicoQuant were upgraded and integrated into one complete system. Then customized software developed in LabVIEW controlled the hardware and handling of the samples.

Potential sample types were reviewed and both single crystal and polycrystalline CdTe were chosen for this project. The single crystal samples also varied by depositing a passivation layer of ZnO on one side of the wafer. Also, the single crystal samples experienced two different types of wet chemical cleans involving with or without a dipping into hydrochloric acid (HCL).

The final and most important aspect as well as the main focus of this thesis was generating analysis software in Matlab to read the TRPL curves and extract the desired parameters. After the raw curves were collected and stored into an array the Matlab

analysis software would then read the data and start the process of extracting the parameters. Multiple sub-routines were written in Matlab to create the main program in order to extract the S_f, S_b, μ, and τ parameters. These sub-routines and main code along with the numerical methods will be explained in further detail in the chapter 5.

4.2 Hardware Setup / Overview

In order to create the photon excitation of the CdTe, the equipment used a 641 nm picosecond pulsed laser diode, controlled by a picosecond pulsed diode laser driver (PDL). The 641 nm laser is used to only excite the CdTe and should not be absorbed by the CdS or the ZnO layer. The PDL has base frequency range of 80 MHz (PicoQuant, n.d.). This base 80 MHz frequency is divided by the repetition frequency dial's value that was set to 8. This setting equates to a laser pulse trigger of 10 MHz for all measurements. The pulse width of the laser was 50 ps at full width half max (FWHM) [17].

After the CdTe became excited by the laser pulse, the photons given off were collected by PicoQuant's PDM series "Single Photon Avalanche Diodes", manufactured by Micro Photon Devices (MPD) [17]. The silicon Single Photon Avalanche Diode (SPAD) was "specifically designed and optimized for time-resolved photon counting applications" such as TRPL [17]. The SPADs provided a photon timing resolution of almost 84ps at FWHM [17]. The exact pulse width of the hardware was observed inside the instrument function (IRF) curve and later convoluted from the sample measurement curve. The SPAD collected the photons and communicated the information to the

PicoHarp300, which stored the count with a time stamp. The counts were then displayed in FluoFit software [17]. FluoFit is the generic software provided by the vendor to control the PicoQuant hardware. All PicoQuant base hardware along with their software can be found at www.picoquant.com. An example of the basic hardware setup can been seen in the figure below:

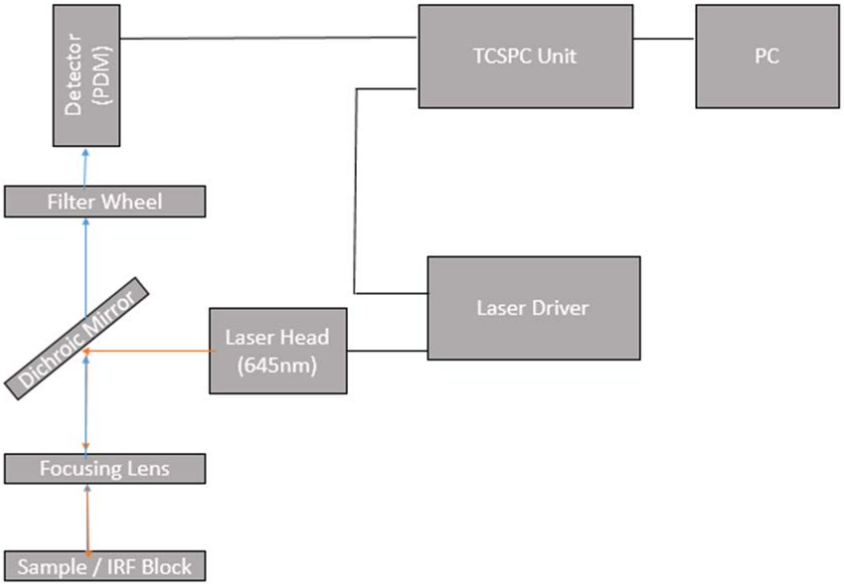

Figure 4-1: Typical setup for a TRPL system

The TRPL used has gone through a few upgrades before the sample measurements were collected. Linear stages were added to provide automatic focusing capabilities of the laser light on the sample. They also provide the ability to easily map out measurements across the sample in an automated fashion. A light tight enclosure was built to prevent any outside light from affecting the IRF, sample measurement and saturation of the detector. This enclosure contained all of the equipment except for the computer. Micro-manipulators were added as mounting to fiber coupler to provide laser

alignment through the dichroic mirror and onto the sample. Automatic filter wheels with long pass filters were added to the system in order to control which wavelength of light will reach the detector. An automatic neutral density filter was used to evenly cut the signal down in order to not saturate the detector. The detector was mounted on top of micro-manipulator stage. This aided in optimizing the alignment which maximized the incoming signal from the CdTe.

The hardware used the following setup for all of the measurements shown in the table below.

Table 4.1: Hardware specifications used before any measurements were taken

TRPL Hardware Setup:					
Sample:	Time Resolution (psec)	Laser Rep.Freq (MHz)	Laser Wavelength (nm)	Total Counts (unit less)	Max Optical Power (mW)
IRF	16	10	641	20,000	1.5
Sample A	16	10	641	20,000	1.5
Sample B	16	10	641	20,000	1.5
Sample C	16	10	641	20,000	1.5

Sample C is the polycrystalline sample with working devices. Sample A is the single-crystal CdTe without the HCL bath. Sample B was the single-crystal CdTe with the HCL dip.

4.3 Software Setup / Overview

The TRPL measurement was automated using LabVIEW. LabVIEW software that was created for controlling all the PicoQuant equipment along with automated filter

wheels and stages. The LabVIEW program called PicoQuant's dll in order to provide similar hardware functionality as the FluoFit software did. The Picoharp dll provided the functionality to set the time resolution and the total counts to be collected and calculate the repetition frequency for each scan. The time resolution is needed in order to determine the spacing on x axis. This is required since the counts are collected by timestamp. The total counts function provides the LabVIEW software with a stop condition once the desired number of counts are received. The standard counts stop condition was set to 20,000 data points. The program could also scan the sample in multiple locations and verify that the laser was in focus based upon the samples working height and feedback intensity. The LabVIEW program also controlled the filter wheels and would choose the proper filters based upon if IRF or a sample scan was selected. The TRPL program provided the ability to record and save sample information and raw data, along with displaying the counts of the TRPL measurements in real time.

4.4 Instrument Response Function

Before any sample measurement could be taken, an IRF must first be collected. A special light scattering block provided by PicoQuant was used for collection of the IRF. It is better to use this material instead of just aluminum to prevent saturation signal on the detector. This IRF block scatters the laser light and some of the scatter is collected by the detector to determine the hardware's response time. The automatic filter wheels were set to allow the laser wavelength through to the detector. Once the IRF was collected the 90 ps FWHM could be seen. An IRF was collected before and after each set of samples ran.

This was just a precautionary way of verify the system is not drifting over time. This IRF data will be used later by the Matlab analysis software.

4.5 Sample Preparation / Measurement Location

4.5.1 Polycrystalline CdTe

The first set of measurements came from the patterned dot-cell looking polycrystalline sample. This was polycrystalline CdTe sample that was previously described in this study in chapter 3, device structure. Going forward I will refer to this sample as "Sample C". Sample C's measurements were broken down into two categories based upon sunny or film side measurements. The sunny-side where the glass is facing up toward the incoming laser and the film-side is laying on the stage platform as shown in the figure below:

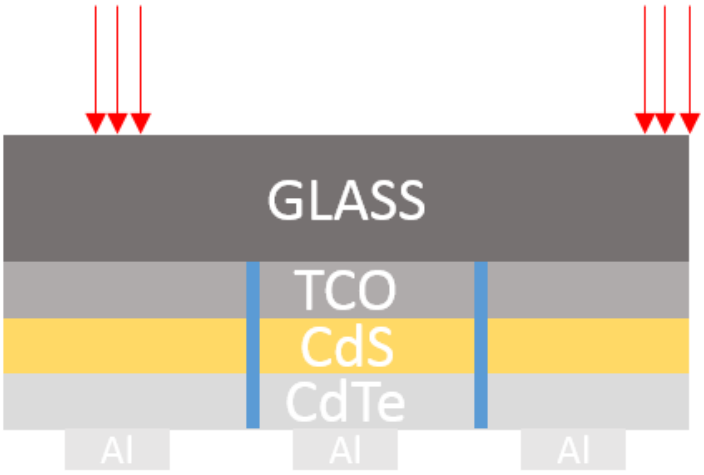

Figure 4-2: Polycrystalline sunny side orientation

The film side measurements had the CdTe film facing upwards toward the incoming laser and the glass substrate is on the bottom laying on the stage platform. This setup looks like the figure below.

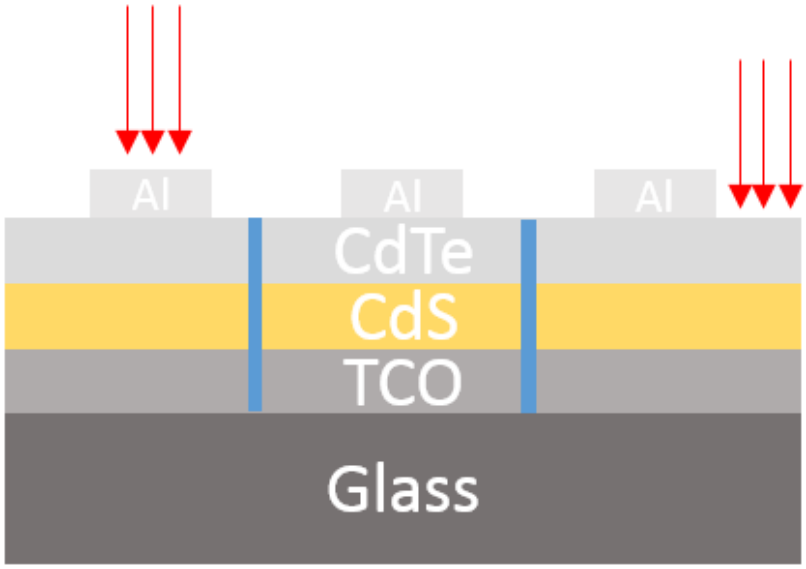

Figure 4-3: Polycrystalline film-side orientation

The measurements for Sample C were broken down even further into two categories of measurements on the metal contact pad and between cell where there was no metal just the CdTe and CdS interface shown by the arrows in the Figures 4-2 and 4-3 above. This process was repeated by collecting many measurements across the sample in order to provide a mapping and verification of the data. One difficult aspect with this sample was determining when the measurement was on or in-between cells but not on the soldered scribe lines when the sunny side to sample was facing the laser. Later the raw counts data for both the IRF and sample were copied to an excel data sheet, which the analysis software would then analyze.

4.5.2 Single-crystal CdTe

The single crystal samples had a slightly different approach. They required an organic clean and then needed to have the passivation layer deposited on them. Going forward I will refer to the single crystal samples as “Sample A” and “Sample B”.

The single crystal samples were then separated out from each based upon the type of organic clean they received. The clean process is shown in the following table.

Table 4.2: Organic cleaning specifications

Single Crystal Clean				
Sample:	Acetone Bath (min)	Isopropyl Alcohol (sec)	Hydrochloric Acid (sec)	Deionized Water (min)
Sample A	5	60	0	0
Sample B	5	60	30	5

Both samples A and B were dipped into an ultrasonic Acetone bath for 5 minutes to clean off any glass or debris that might be at the surface. Then they were both washed with agitated Isopropyl alcohol bath to clean off the Acetone. Dried off with clean dry air for a few seconds, till the film no longer showed any residue on it. Sample B was then dipped into a 1:10 ratio of HCL for 30 seconds. Afterwards, the HCL was washed off by deionized water for 5 minutes to ensure there would be no residue of the acid left at the surface of the CdTe. The sample was then dried by clean dry air.

After the organic clean was finished both sample A and B had the passivated layer of ZnO deposited. The room temperature ZnO was applied at a rate of 20 Å per minute for 10 minutes to achieve a layer thickness totaling 200 Å.

Once the deposited film was finished the samples were measured on the TRPL equipment. The measurements were taken on both sides in order to measure the open CdTe surface and at the interface between the ZnO and CdTe layer. One example of the orientation for the measurements looked similar to Figure 4.4 below.

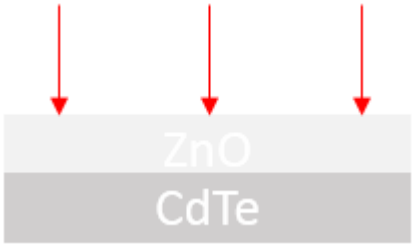

Figure 4-4: Single crystal samples' orientation to the laser light path

The measurement specs for both sample A and sample B follow the values that are in Table 4.1 in this chapter. As seen in Table 4.1 the hardware was able to measure both technologies without having to alter the settings. All TRPL measurements were taken at First Solar using their equipment. Data for these measurements including IRF's were also separated out inside individual excel sheets for the analysis software to use.

Chapter 5

Analysis Software and Quantitative Methods:

5.1 Analysis Software Introduction

After all measurements have been taken the analysis software can then be used to look at the raw data collected. The analysis software can be broken down into a few main sections that were written in Matlab. The main code called TRPL.m, calls multiple sub-functions and has the ability to change the materials parameters based upon the type of sample to be analyzed. A copy of the main code can be found in Appendix A: Main – Program. The parameters that need to be adjusted ahead of time depending on which type of CdTe was analyzed are as follows:

1. Absorber thickness
2. Initial guess parameters:
    a. S_f
    b. S_b
    c. μ
    d. τ

e. Bkg

3. Upper and Lower Boundary conditions for each parameters
4. Xmesh value

This chapter will step through the main TRPL.m program and its sub-functions in sequential order along with describing the quantitative methods used in the specific functions. The major parts of the code had comments left after the lines that explains what is happening. These comments can be found by looking at the appendix of this study at the raw code.

5.2 Software Outline

The analysis main code can be broken down into a few major parts, these can be seen in Figure 5-1. The flow chart below, briefly describes the major functions and process flow the analysis code uses. These functions are called at the top of the flow chart then work down through where the final solution is extracted.

The fitting procedure can also be broken down into many sub-functions. Figure 5-2 below shows the order of operations in which the sub-functions are called starting at the bottom first, then looping through n-number of times.

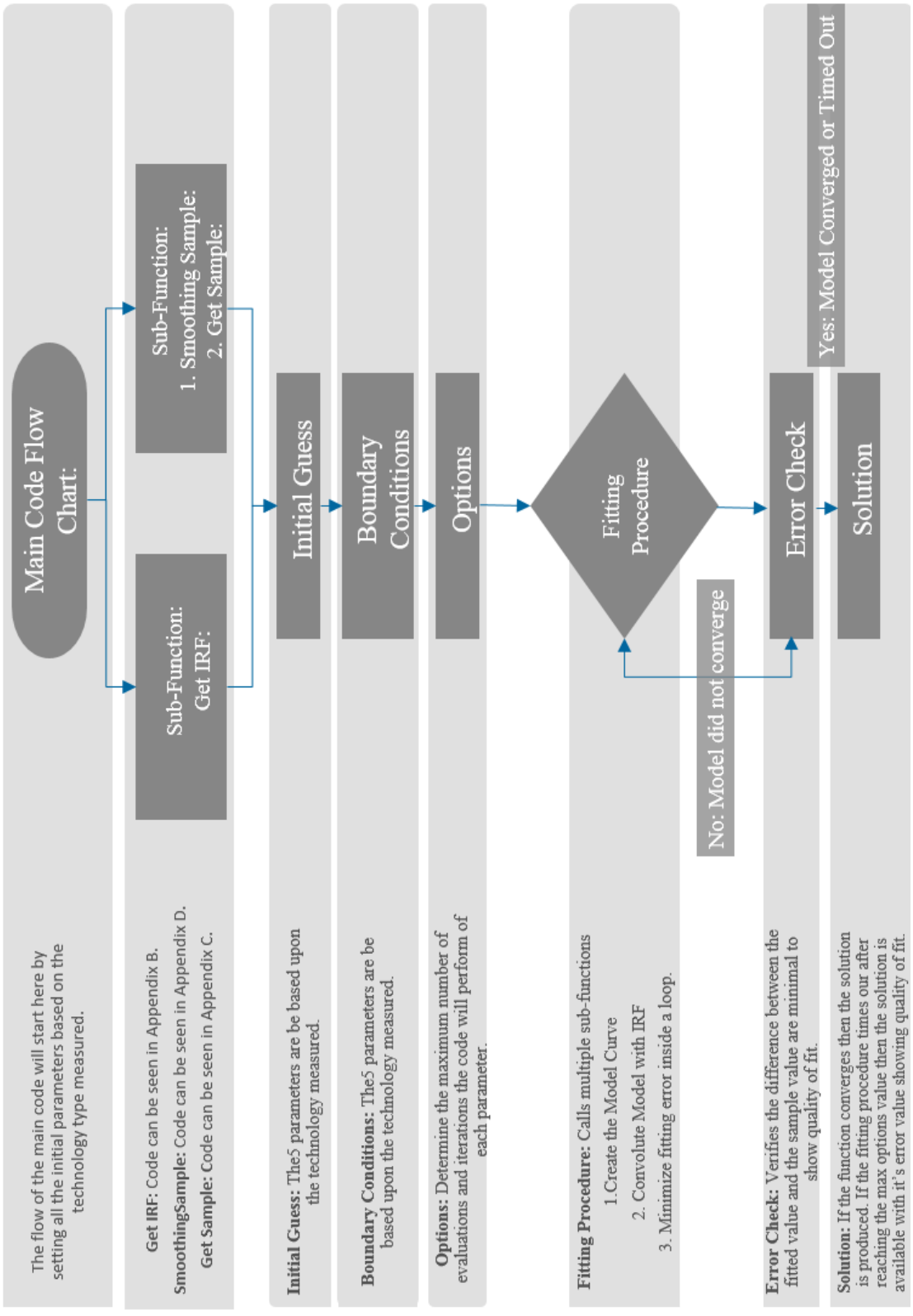

Figure 5-1: Flow chart shows the main codes

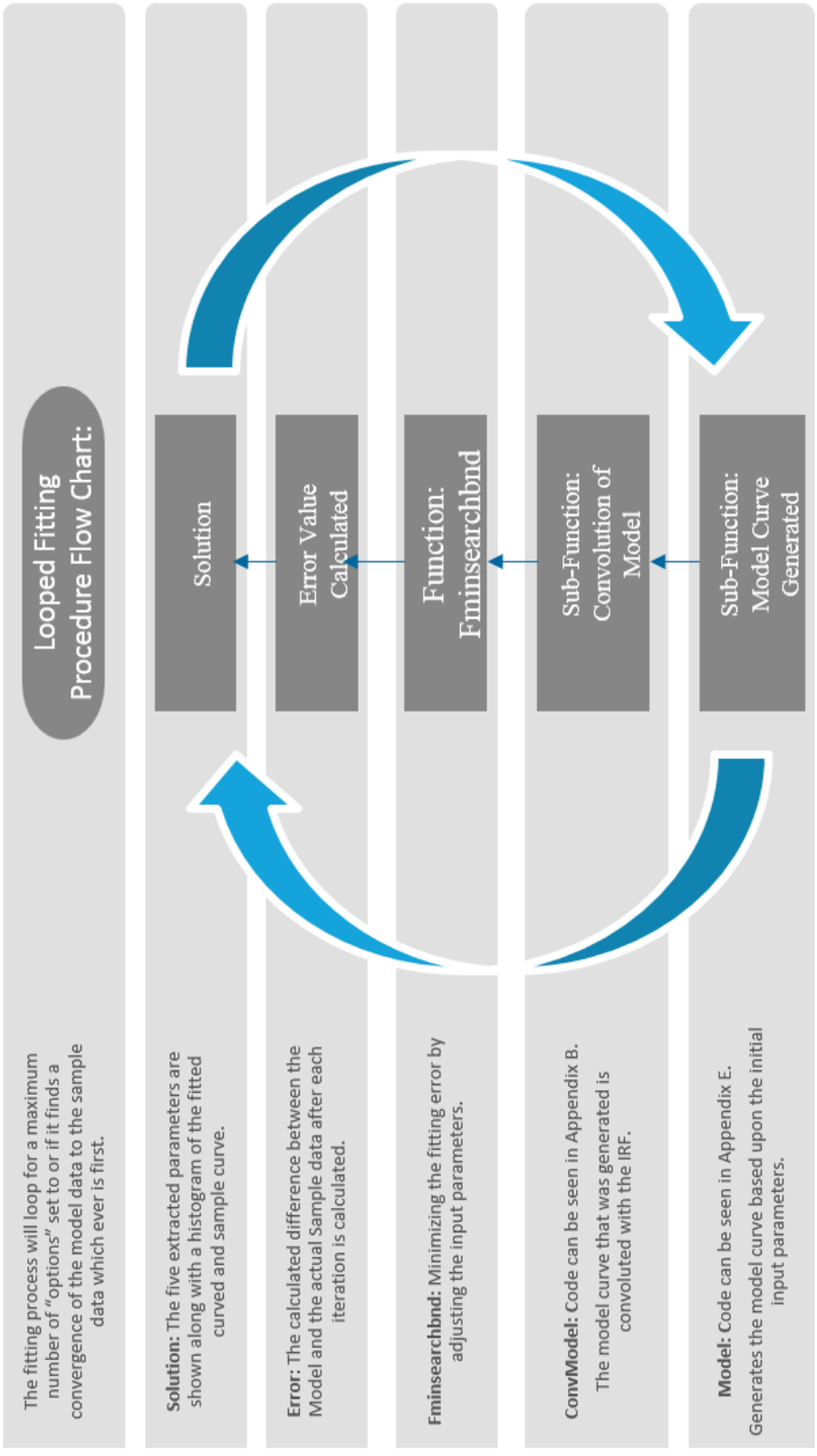

Figure 5-2: The looped fitting procedure

As seen in the Figure 5-1 flow chart, the main program was broken down into multiple sub-functions. The main program “TRPL” is found in Appendix A, and calls the multiple sub functions. The “getIRF” function is in Appendix B and collects the IRF of the instrument. The “getSample” function is in Appendix C and collects the Sample TRPL raw measurement then calls the “SmoothingSample” function in Appendix D. Next the user defined parameters initial guess, boundary conditions, and options are called. The fitting procedure starts next as seen in Figure 5-2. Inside the loop, the first function called is the “Model” found in Appendix E. This function generates the fitted curve based upon the user defined parameters. That fit is then convoluted with the IRF of the instrument by the function “ConvModel.m” found in Appendix F. The main “TRPL” code then uses the Matlab built in function “fminsearchbnd” to minimize the error. Afterwards, either a solution was found by the function converging or a timeout of the software would occur. All functions can be seen in more detail inside the appendixes of this study.

5.3 Assumptions for Calculations

Before beginning with the quantitative methods, the work can be broken down into a few key assumptions:

1. It is assumed that the TRPL is taken in a high injection level (HIL).
    a. The device under test stays in this HIL state for the entire duration of the measurement.

b. Another assumption is the laser provides enough power to create the HIL condition.

2. Since the measurement is taken in HIL, solving these equations assumes that the minority and majority carriers will combine and are measured as an electron hole pair.
    a. The electron hole pairs are calculated as one particle that is neutral in charge.
    b. This leads to not having to solve for election or hole mobility but particle ambipolar mobility.
3. It also assumes that all current is based upon diffusion, because of minimal to no electric field in the quasi neutral region.
    a. Which simplifies the equations used and we can ignore Poisson's equation.
4. The Sb was pinned for the single crystal because there was no metal contact at the either side of the device, so it is presumed to be at thermal velocity 10^7 cm/s. [28]
5. We assume the background (Bkg) or noise of the TRPL equipment to be a time independent variable.
    a. The noise is considered to be at a constant level inside the equipment and is added back into the convolution and the log scale fitted curve.

5.4 Quantitative Methods

As discussed in previous chapters, time-resolved photoluminescence is a technique that effectively measures decay of PL intensity as a function of time after initial laser excitation. In the pure semiconductors, photoluminescence is caused predominantly by band-to-band transitions resulting in energy release in the form of photon. Since transition of an electron from the conduction to the valence band could be considered as bimolecular reaction between electron and hole, the rate of such transitions is proportional to the concentrations of both carriers. Moreover, band-to-band transitions occur at different depths of semiconductor layer, so that the total PL intensity could be found at any time as:

$$I(t) = B\int_0^d n(x,t)\, p(x,t)\, dx \tag{5.1}$$

In (5.1) B represents radiative rate constant.

In order to determine free carrier profiles that enter equation (5.1), we need to consider what happens in semiconductor layer after initial excitation.

After the laser pulse is terminated, evolution of free carrier profiles is governed by general diffusion-reaction equation, better known in semiconductor physics as the continuity equation:

$$\begin{cases} \dfrac{dn}{dt} = -\nabla J_e - R \\ \dfrac{dp}{dt} = -\nabla J_h - R \end{cases} \tag{5.2}$$

In (5.2), J_n and J_p represent fluxes of electrons and holes, respectively, and R stands for the net recombination rate. In general, the flux of a charged species X in the gradient of

electrochemical potential is defined by its concentration $[X]$, diffusivity D_X, and the gradient of its electrochemical potential $\nabla\mu_X$:

$$J_X = -\frac{D_X}{kT}[X]\nabla\mu_X \tag{5.3}$$

Then, flux expressions for electrons and holes could be derived for their electrochemical potentials as:

$$\begin{cases} J_e = -\dfrac{D_e}{kT} n\nabla\mu_e = -\dfrac{D_e}{kT} n\nabla\left(-\chi - qV + kT\ln\left(\dfrac{n}{N_C}\right)\right) \\ J_h = -\dfrac{D_h}{kT} p\nabla\mu_h = -\dfrac{D_h}{kT} p\nabla\left(\chi + E_G + qV + kT\ln\left(\dfrac{p}{N_V}\right)\right) \end{cases} \tag{5.4}$$

Since we only consider evolution of photo-generated profiles in absorber with uniform band structure, (5.2) could be simplified as:

$$\begin{cases} J_e = -D_e n\nabla\left(-\dfrac{q}{kT}V + \ln n\right) \\ J_h = -D_h p\nabla\left(\dfrac{q}{kT}V + \ln p\right) \end{cases} \tag{5.5}$$

Finally, assuming uniform diffusion parameters, inserting (5.5) into (5.2) yields:

$$\begin{cases} \dfrac{dn}{dt} = D_e\nabla\left[n\nabla\left(-\dfrac{q}{kT}V + \ln n\right)\right] - R \\ \dfrac{dp}{dt} = D_h\nabla\left[p\nabla\left(\dfrac{q}{kT}V + \ln p\right)\right] - R \end{cases} \tag{5.6}$$

Although simplified, equations (5.6) still presents significant challenge for a numerical solution. We can further simplify the problem set when assuming that high level injection (HLI) persists in absorber during the measured decay. In this case, when injected carrier concentrations greatly exceed the concentration of ionized impurities in semiconductor, charge neutrality is conserved at any point, so that the gradient of electrostatic potential in (5.6) could be neglected resulting in further simplification:

$$\begin{cases} \dfrac{dn}{dt} = D_e \nabla \left(n \nabla \ln n \right) - R = D_e \nabla^2 n - R \\ \dfrac{dp}{dt} = D_h \nabla \left(p \nabla \ln p \right) - R = D_h \nabla^2 p - R \end{cases} \tag{5.7}$$

Moreover, since under HLI conditions, electron and hole concentrations follow each other closely, we may introduce electron-hole pair as a neutral quasi-particle, and rewrite (5.7) for the concentrations of electron-hole pairs $c(x)$ as:

$$\frac{dc}{dt} = D_c \nabla^2 c - R \tag{5.8}$$

Note that equation (5.8) could be obtained directly from (5.7) by equalizing electron and hole concentrations so that $n \equiv p \equiv c$, taking the sum of the equations, and dividing both sides by the factor of two. Then diffusion constant D_c simply represent the average of electron and hole diffusion constants:

$$D_c = \frac{D_e + D_h}{2} \tag{5.9}$$

We can also introduce effective lifetime τ such that $R = \frac{c}{\tau}$, which gives equation (5.8) its final form:

$$\frac{dc}{dt} = D_c \nabla^2 c - \frac{c}{\tau} \tag{5.10}$$

In order to solve parabolic partial differential equation (5.10), we need to define initial and boundary conditions. Assuming the laser pulse is short enough to neglect diffusion of free carriers, initial concentration profile of photo-generated electron-hole pairs is proportional to the flux of photons in semiconductor that decays exponentially as a function of penetration depth:

$$c(x,0) = c_0 \exp(-\alpha x) \tag{5.11}$$

Neumann boundary conditions to equation (5.10) could be derived by introducing surface recombination velocity as proportionality coefficient that at any time t links the flux of electron-hole pairs toward boundaries with their boundary concentrations:

$$\begin{cases} -J(0,t) = D_c \nabla c(0,t) = -S_L c(0,t) \\ J(d,t) = -D_c \nabla c(d,t) = -S_R c(d,t) \end{cases} \tag{5.12}$$

After solving for the ideal PL intensity as a function of time (5.1), convolute it with the IRF measured and add in the background noise as initial guess to create the real fitted PL intensity:

$$I_{FIT}(t) = IRF(t) \otimes I_{PL}(t) + I_{Noise} \tag{5.13}$$

Matlab has a built-in function that will convolute the data automatically. Convolution of the modeled curve with the IRF represents the area of overlap under the two points as the modeled curve slides across the IRF. The model curve data point is multiplied by its counterpart data point from the IRF. Then it adds the elements together during the sliding along the x axis. It does this process until it reaches the end of the modeled curve. Afterwards we assume the noise to be a time independent variable. The noise is considered to be at a constant level inside the equipment and is added back in the log scale fitted curve.

The calculated I_{FIT} from equation (5.13) gets subtracted from the measured decay and the fitting error is calculated as a norm of residuals:

$$E(\tau, \mu, S_F, S_B, d, I_{Noise}) = \left\| PL_{Measured}(t) - I_{Fit}(\tau, \mu, S_F, S_B, d, I_{Noise}) \right\| \qquad (5.14)$$

The target function (5.14) error value is minimized by adjusting the input parameters automatically using Matlab's optimization function "fminsearchbnd". The "fminsearchbnd" function will start with the initial guess parameters and adjust them accordingly while working between the given preset bounds defined at the beginning of the software. Once the minimum error value is reached or the timeout state is reached the solution for each input parameter is extracted.

Chapter 6

Results:

6.1 Results Introduction

TRPL raw data curves were stored into arrays in excel and segregated by the technology type. Afterwards, the analysis software ran for each individual measurement. The data was extracted and compiled into their respective tables to be analyzed. The analysis processed each individual TRPL measurement and the extracted data was saved in tables along with their respective curves.

The test plan layout is seen below in Table 6.1.

Table 6.1: Test plan for extracting results.

Test Plan						
Technology:	Treatment:	Measurement Side:	Test 1:	Test 2:	Test3 :	Test4:
Single-Crystal CdTe	No HCL Clean	CdTe Side Up	1a	1a	x	x
Single-Crystal CdTe	No HCL Clean	ZnO Side Up	1a	2a	x	x
Single-Crystal CdTe	With HCL Clean	CdTe Side Up	2a	1a	x	x
Single-Crystal CdTe	With HCL Clean	ZnO Side Up	2a	2a	x	x
Polycrystalline CdTe	None	CdTe Side Up	x	x	1a	x
Polycrystalline CdTe	None	Sunny Side Up	x	x	1a	x
Polycrystalline P-Type Si Waffer	None	Polished Si Side Up	x	x	x	1a

For each test, data from 1a was compared against 1a and 2a against 2a, the x meant data was not used in that specific test. It was done this way in order to easily see

any performance difference based upon the technology used, cleaning process, and passivation layer comparison. Then the p-type Si wafer was used as a sanity check. The results for each test will be broken down into further detail in the next few sections of this chapter.

The analysis software requires a few key parameter to be chosen before starting the analysis. These are as follows:

1. Type of CdTe:
    a. Polycrystalline or Single-crystal CdTe
2. Absorber thickness
3. Initial guess parameters:
    a. S_f
    b. S_b
    c. μ
    d. τ
    e. Bkg
4. Upper and Lower Boundary conditions for each parameters
5. Xmesh value

6.2 Results and Observations

6.2.1 Single-crystal CdTe without Acid Dip

The single-crystal CdTe, no acid clean, (Sample A) with the CdTe surface facing upwards toward the laser, fit was generated first. The fit can be seen in Figure 6-1 below.

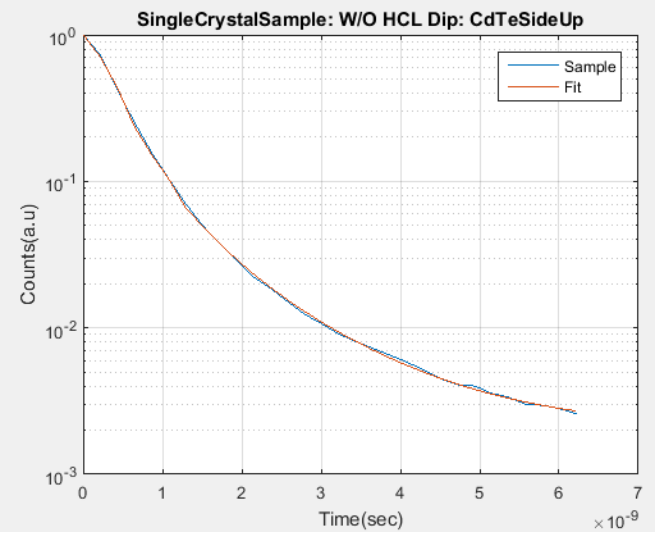

Figure 6-1: Sample A with its fit, CdTe film facing upward

The next fit shows the same device flipped upside down with the absorber facing away from the laser in Figure 6-2.

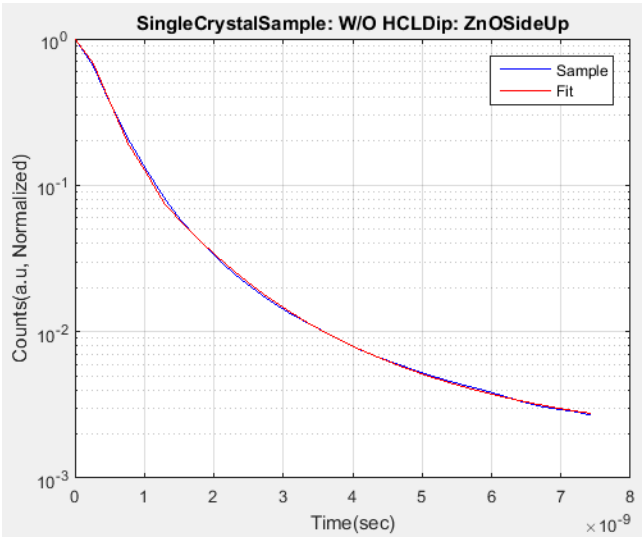

Figure 6-2: Sample A with its fit, ZnO film facing upward

Both fits look visually good as they match up well in the S_f region of the curve. The extracted results from this test are shown in Table 6.2 below.

Table 6.2: Extracted parameters of sample A

Single Crystal: Non-HCL Dip						
	Measurement Side	Error	Sf	Sb	Mu	Tau
Sample:		(%)	(cm/s)	(cm/s)	(cm2 / (V*s))	(sec)
Sample A	CdTe Side Up	0.203	6.60E+04	1.00E+07	485.5	4.40E-09
Sample A	ZnO Side Up	0.164	5.90E+04	1.00E+07	490	5.00E-09

As we can see by pinning the S_b parameter, the percent error for the overall fit compared to that of the sample measurement was a reasonable 0.164% and 0.203%. All of the extracted parameters are within the values described in chapter 2 Background information of this thesis. Interesting enough, there is no major benefit on this sample for adding on the ZnO passivation layer. The only advantage seen, was a slightly slower S_f velocity with a slightly higher τ.

6.2.2 Single-crystal CdTe with Acid Dip

The single-crystal CdTe, with HCL clean, (Sample B) CdTe was compared next. The CdTe surface facing upwards towards the laser, fit can be seen in Figure 6-3.

Figure 6-4 shows a much steeper slope in the front of the curve than Figure 6-3. This steeper slope relates to the surface recombination velocity. Also, the longer lifetime of this sample is evident when looking at the two curves.

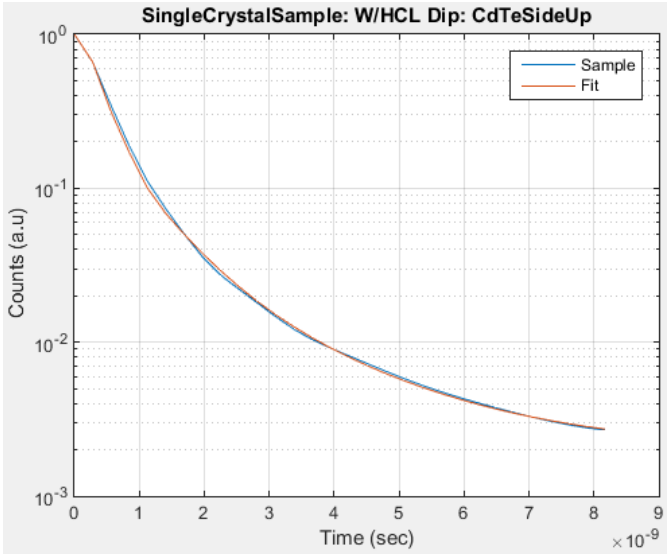

Figure 6-3: Sample B with its fit, CdTe film facing upward

The same sample only flipped with the ZnO surface facing the laser fit can be seen in Figure 6-4.

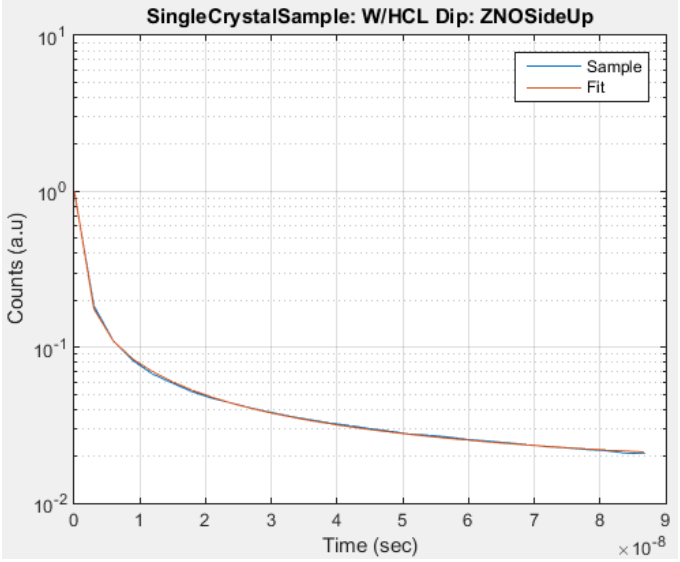

Figure 6-4: Sample B with its fit, ZnO film facing upward

Table 6.3 extracted parameters below shows these claims to be true.

Table 6.3: Extracted parameters of sample B

Single Crystal: HCL Dip						
	Measurement Side	Error	Sf	Sb	Mu	Tau
Sample:		(%)	(cm/s)	(cm/s)	(cm2 / (V*s))	(sec)
Sample B	CdTe Side Up	0.224	5.60E+04	1.00E+07	497	5.30E-09
Sample B	ZnO Side Up	0.096	7.20E+03	1.00E+07	284.6	4.50E-07

As seen in Table 6.3, sample B with the ZnO layer facing upwards toward the laser has the longer τ and with slower S_f and μ. This could due to the combination of passivation layer with the HCL clean. It is known that chlorine will bond with the CdTe and will clean up the surface by getting rid of recombination centers. As previously stated in the background chapter mobility is also heavily dependent upon the doping of the material. So the doping of HCL could be affecting the mobility. This affect is only seen with the addition of the passivation layer as well. When comparing similar sides of both sample A and sample B, the same conclusions drawn from above can be seen in Table 6.4.

Table 6. 4 Sample A versus Sample B

Single Crystal CdTe Side Comparision						
	Measurement Side	Error	Sf	Sb	Mu	Tau
Sample:		(%)	(cm/s)	(cm/s)	(cm2 / (V*s))	(sec)
Sample A	CdTe Side Up	0.203	6.60E+04	1.00E+07	485.5	4.40E-09
Sample B	CdTe Side Up	0.224	4.60E+04	1.00E+07	497	5.30E-09
Sample A	ZnO Side Up	0.164	5.90E+04	1.00E+07	490	5.00E-09
Sample B	ZnO Side Up	0.096	7.20E+03	1.00E+07	284.6	4.50E-07

Then plotting the similar sides against each other can be seen in Figure 6.5.

Unfortunately, since the performance between Sample A and B's ZnO side was so drastic, they could not be plotted together to visually see the difference. They were unable to align to the same axis.

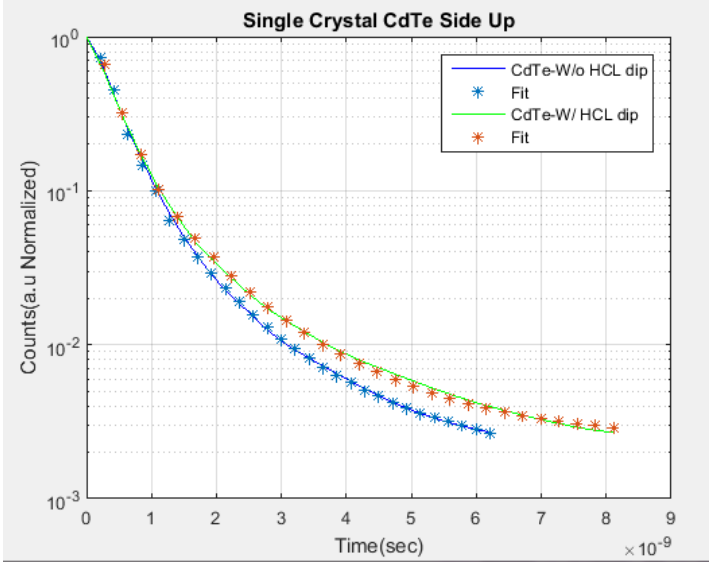

Figure 6-5: Sample A & B; with and without HCL clean with CdTe facing upwards

6.2.3 Polycrystalline CdTe

The last of the CdTe samples that were measured was the polycrystalline CdTe (Sample C). The fit looks compared to the actual measured sample can be seen in Figure 6-6 which shows the CdTe side up and Figure 6-7 which shows the Glass Side up.

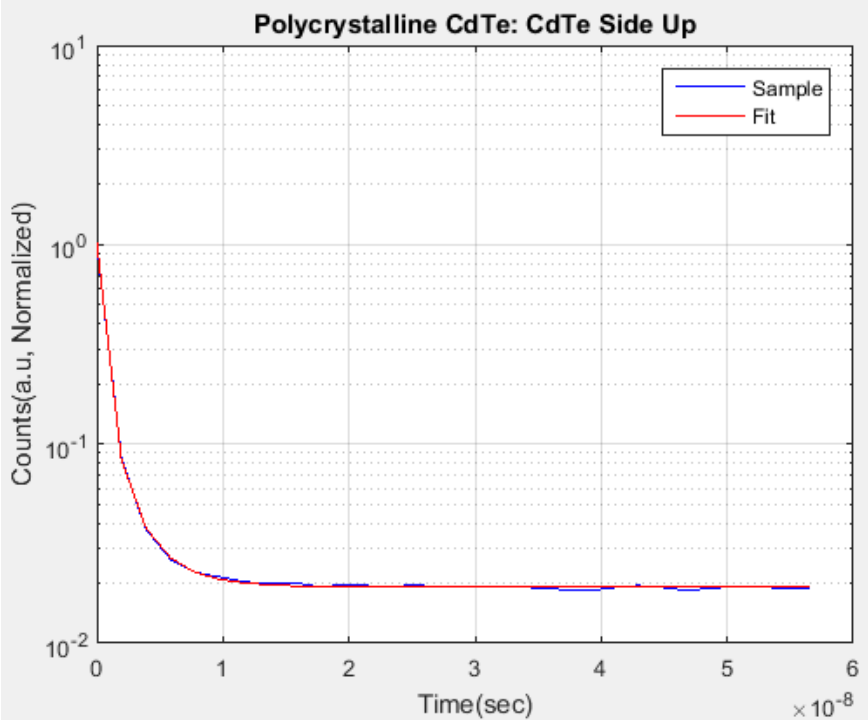

Figure 6-6: Sample C with its fit, CdTe film facing upward

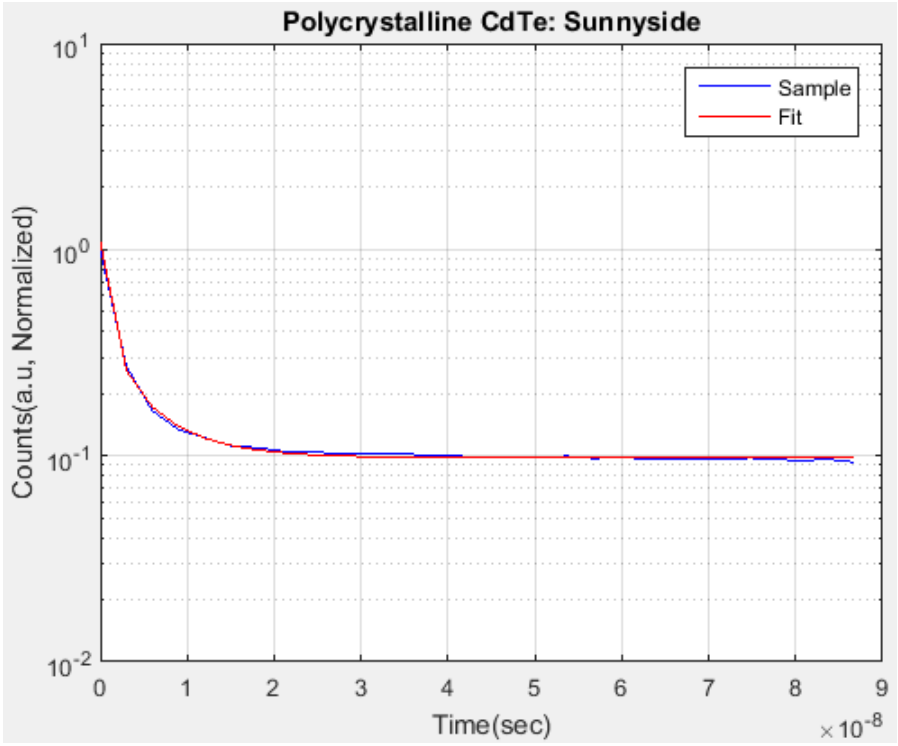

Figure 6-7: Sample C with its fit, glass side facing upward

The fits look fairly similar to each other with slight difference in S_f seen. The lifetimes are flatten out pretty quickly after 10 ns and 18 ns respectively. Table 6.5 below shows the extracted parameters from sample C.

Table 6.5: Extracted parameters sample C

Polycrystalline CdTe:						
	Measurement Side	Error	Sf	Sb	Mu	Tau
Sample:		(%)	(cm/s)	(cm/s)	(cm2 / (V*s))	(sec)
Sample C	CdTe Side Up	0.102	1.20E+04	5.00E+06	20	1.00E-08
Sample C	Sunny Side Up	0.168	8.00E+03	7.75E+06	20	1.80E-08

These values line up reasonably well with what was published in the research papers talked about in the background chapter of this study. The mobility is a little on the lower side but is still reasonable considering this is polycrystalline CdTe. The ranges found suggested it to be around 50 (cm^2 / (V*s)) or greater. But once again that depends on doping and other external mechanisms added. The other measurements around this sample also produced similar mobility's. Electron lifetimes of 10-30 ns for p-type polycrystalline CdTe have been reported. [29] The extracted values for this sample falls in that range. The Sunny side with the passivation layer of CdS does show better overall performance compared to that of just the CdTe surface.

6.2.4 All CdTe Samples

Table 6.6 below shows all the data collected for an easier view of the different technologies performance.

Table 6.6: Single-crystal versus polycrystalline CdTe

Single Crystal CdTe vs. Polycrystalline CdTe						
	Measurement Side	Error	Sf	Sb	Mu	Tau
Sample:		(%)	(cm/s)	(cm/s)	(cm2 / (V*s))	(sec)
Sample A	CdTe Side Up	0.203	6.60E+04	1.00E+07	485.5	4.40E-09
Sample A	ZnO Side Up	0.164	5.90E+04	1.00E+07	490	5.00E-09
Sample B	CdTe Side Up	0.224	5.60E+04	1.00E+07	497	5.30E-09
Sample B	ZnO Side Up	0.096	7.20E+03	1.00E+07	284.6	4.50E-07
Sample C	CdTe Side Up	0.102	1.20E+04	5.00E+06	20	1.00E+08
Sample C	Sunny Side Up	0.168	8.00E+03	7.75E+06	20	1.80E-08

Nothing to alarming stands out between all the various samples that has not already been discussed. Similar to that of the ZnO passivation layer when the CdS layer was facing the laser there was a performance improvement compared to that of just CdTe bare surface. The mobility inside sample A and B is faster than sample C, this can be attributed to grain boundary scattering of the polycrystalline CdTe. [15]
Both sample A and B used a mesh value of 20 and sample C used 15 as its optimized value. This enabled the percent error value to be as low as possible.

6.2.5 Silicon Wafer

A p-type polysilicon wafer was also tested in order to provide an additional sanity check to the values extracted from the CdTe samples. This measurement was taken, but the generated TRPL curve was the IRF of the instrument. The lack of generated curve could be due to a few reasons. The polysilicon wafer is an indirect band gap material making it much harder to generate a photon. The TRPL hardware itself is optimized to only measure CdTe and not silicon. No fit was generated due to the inability to accurately measure the TRPL of the silicon wafer.

6.2.6 Observations

During the analysis evaluations, it was seen that altering the xmesh values on the PDEPE solver greatly affect the fit quality and extracted values. Xmesh is a built in function inside Matlab's PDEPE solver and will greatly affect the solving time and final solution. Xmesh describes the point spacing that was used between points on the modeled curve generated. The value was determined by using a guess and check approach. Which means having to manually vary the xmesh value up and down multiple times. Eventually, an ideal value for xmesh was found for each type of CdTe. The fit was verified by looking at the generated histograms fit versus the sample measurement, as well as having the lowest extracted error value for each solution. The final ideal xmesh values found, ranged between 15 for polycrystalline and 20 for single-crystal CdTe.

The analysis software roughly took a little over a minute and half to analyze one side of a sample. Keeping in mind that the xmesh value used greatly affects the processing time of the analysis software.

The IRF was taken before any measurement was started and then taken again at the end of all measurements to verify there was no drift in the system. This also made it easier for there to be only one required IRF for all measurements to be convoluted with.

6.3 Software Limitations

Furthering the robustness of the process of extracting the parameters from the TRPL measurement would be beneficial when dealing with different technologies or

photovoltaic films. Having a way to call upon the input parameters automatically based upon the technology that is being tested would save time. An upgrade to the software that would implement an automatic procedure to vary the nmesh size would help to improve the accuracy of the fit. Also, the measurement technique itself could vary results based upon the laser wavelength and type used. Changing the wavelength of the laser could lead to extracting other layers besides just the CdTe. The last limitation of this software would be able to handle low injection level TRPL instead of only HIL.

Chapter 7

Conclusion and Future work:

7.1 Summary and Conclusion

As seen from the results' section the analysis software generated reasonable and reliable fits that modeled the samples' raw data. This study confirmed that taking advantage of the TRPL measurement technique does prove to be a viable way to extract material parameters such as S_f, S_b, μ, and τ. It also provided evidence that the developed software is an effective addition to the analysis of any HLI TRPL measurement.

Out of the various single crystal samples the side with the addition of the ZnO passivation layer versus the bare CdTe surface resulted in higher performance. The data showed this by the longer lifetimes and the slower surface recombination rates. The HCL clean on the single crystal sample also proved to help in the performance of the material. The HCL acted as a fluxing agent in order to improve the surface between the ZNO and the CdTe. The single crystal sample that had the HCL clean clearly showed a much longer lifetime than that of its counterpart sample, represented in the figures in the

results' section of this study. The higher performance shown in the cleaned sample is a result from the removing of defects inside the absorber material.

The most significant part of this study was being able to prove that S_f, S_b, μ and τ parameters can be extracted from the TRPL measurement. The analysis software was able to consistently read the TRPL curve and generate an accurate fit, along with extracting the fit parameters. These values could be seen in the results chapter and reasonably matched up with viable ranges found in various research papers for each parameter. Those ranges were found and discussed inside the background chapter of this study. It is important to keep in mind when comparing the extracted solutions to the published ranges the sample preparation and temperature of sample will vary the values greatly. Having a target range is key since it provides the way of validating the software. The extracted parameters of this experiment also had a percent error associated to each fit. This percent error ensured that the fit was done correctly and the histograms visually showed how close the fit actually was compared to the measured sample.

This new method of extracting the S_f, S_b, μ, and τ will aid engineers and scientists in determining which process is changing their device's performance. This ability leads to more in-depth knowledge of CdTe material. The ability to quickly extract S_f, S_b, μ, and τ makes the case for the importance of incorporating TRPL measurements as a part of standard characterization methods.

7.2 Future Work

In the future, this work can be expanded to include additional aspects of research in this field. One way will be to measure TRPL in a low injection state and extract the same parameters using a similar software technique. Another research aspect would be having software that could switch between the various types of semiconductors using some kind of library for the input parameters needed. Finally, it could be expanded to extract these same parameters by changing laser wavelengths in order to study the various layers of a CdTe solar cell. This could help lead to optimizing the entire solar cell stack.

References

[1] W. Metzger, R. Ahrenkiel, P. Dippo, J. Geisz, M. Wanlass and S. Kurtz, "Time-Resolved Photoluminescence and Photovoltaics," in *2004 DOE Solar Energy Technologies*, Denver , 2005.

[2] S. Jovanovic, G. Devenyi, V. Jarvis, K. Meinander, C. Haapamaki, P. Kuyanov, M. Gerber, R. LaPierre and J. Preston, "Optical characterization of epitaxial single crystal CdTe thin films on Al2O3 (0001) substrates," *Thin Solid Films*, vol. 570 Part A, pp. 155-158, 3 January 2014.

[3] G. Fonthal, L. Tirado-Mejia, J. Marin-Hurtado, H. Ariza-Calderon and J. Mendoza-Alvarez, "Temperature dependence of the band gap energy of crystalline CdTe," *Journal of Physics and Chemistry of Solids*, vol. 61, no. 4, pp. 579-583, April 2000.

[4] C. H. a. S. Bowden, "PVEducation," 27 March 2015. [Online]. Available: http://www.pveducation.org/.

[5] D. Messerschmidt, K. Bratz, W.-M. Gnehr and H. Romanus, "Optical properties of anodically degraded ZnO," *Journal of Applied Pysics* , vol. 115, no. 9, pp. p094902-1-094902-8. 8p, 11 January 2014.

[6] W. Contributors, "Zinc oxide," 13 March 2015. [Online]. Available: http://en.wikipedia.org/w/index.php?title=Zinc_oxide&oldid=651177370. [Accessed 07 April 2015].

[7] W. Contributors, "Solar Energy," Wikipedia, The Free Encyclopedia, 11 April 2013. [Online]. Available: https://en.wikipedia.org/wiki/Solar_energy. [Accessed 20 April 2015].

[8] D. Rose, F. Hasoon, R. Dhere, D. Albin, R. Ribelin, X. Li, Y. Mahathongdy, T. Gessert and P. Sheldon, "Fabrication Procedures and Process Sensitivities for CdS/CdTe Solar Cells," in *Progress in Photovoltaics*, Wiley and Sons, 1999, pp. 331-340.

[9] J. Han, C. Liao, T. Jiang, C. Spanheimer, G. Haindl, G. Fu, V. Krishnakumar, K. Zhao, A. Klein and W. Jaegermann, "An optimized multilayer structure of CdS layer for CdTe solar cells application," *Journal of Alloys and Compounds*, vol. 509, no. 17, pp. 5285-5289, 2011.

[10] S. Demtsu, J. Sites and D. Albin, "Role of Copper in the Performance of CdS/CdTe Solar Cells," in *IEEE 4th World Conference on Photovoltaic Energy Conversion (WCPEC-4)*, Waikoloa, 2006.

[11] S.M.Sze, in *Physics of Semiconductor Devices*, New Jersey, A John Wiley & Sons, INC., 2007, pp. 62-63.

[12] J. Lee, N. Giles, D. Rajavel and C. Summers, "Room-temperature band-edge photoluminescence from cadmium telluride," *The American Physical Society*, vol. 49, no. 3, pp. 1668-1676, 15 January 1994.

[13] R. Dhere, H. Cheong, S. Smith, D. Albin, A. Mascarenhas and T. Gessert, "Micro-PL Studies of Polycrystalline CdS/CdTe Interfaces.," in *NCPV Program Review Meeting*, Denver, 2000.

[14] W. K. Metzger, D. Albin, D. Levi, P. Sheldon, X. Li, B. M. Keyes and R. K. Ahrenkiel, "Time-resolved photoluminescence studies of CdTe solar cells," *Journal of Applied Physics*, vol. 94, no. 5, p. 94, 1 September 2003.

[15] R. Ahrenkiel, N. Call, S. Johnston and W. Metzger, "Comparisonoftechniquesformeasuringcarrierlifetimeinthin-filmand multicrystallinephotovoltaicmaterials," *Solar EnergyMaterials&SolarCells*, vol. 94, p. 2197–2204, 2010.

[16] D. Kuciauskas, J. N. Duenow, A. Kanevce, J. V. Li, M. R. Young, P. Dippo and D. H. Levi, "Optical-Fiber-Based, Time-Resolved Photoluminescence Spectrometer for Thin-Film Absorber Characterization and Analysis of TRPL Data for CdS/CdTe Interface," in *2012 IEEE Photovoltaic Specialists Conference*, Austin, 2012.

[17] "PicoQuant," [Online]. Available: http://www.picoquant.com/. [Accessed 6 April 2015].

[18] J. Duenow, J. Burst, D. Albin, D. Kuciauskas, S. Johnston, R. Reedy and W. Metzger, "Single-crystal CdTe solar cells with Voc greater than 900 mV," *APPLIED PHYSICS LETTERS*, vol. 105, no. 00036951, pp. 1-4, 13 July 2014.

[19] B. Zeghbroeck, "Principles of Semiconductor Devices," 1 January 2011. [Online]. Available: http://ece-www.colorado.edu/~bart/book/. [Accessed 15 September 2015].

[20] J. Nelson, in *The Physics of Solar Cells*, Covent Garden, London, Imperial College Press, 2010, p. 81.

[21] W. Contributors, "Low level injection," 28 November 2014. [Online]. Available: http://en.wikipedia.org/w/index.php?title=Low_level_injection&oldid=635827873. [Accessed 30 March 2015].

[22] P. Mahala, S. K. Behura, C. Dhanavantri, A. Ray and O. Jani, "Metal/InGaN Schottky junction solar cells: an analytical approach," *Applied Physics A Materials Science & Processing*, vol. 118, no. 4, pp. 1459-1468, 9 December 2014.

[23] W. Schockley and J. W.T. Read, "Statistics of the Recombinations of Holes and Electrons," *Physical Review*, vol. 87, no. 5, pp. 835-842, 1 September 1952.

[24] A. Morales-Acevedo, "Thin film CdS/CdTe Solar cells: Rsearch perspectives," in *Solar Renewable Energy News Conference*, Mexico DF, 2005.

[25] T. Gessert, D. R.G., J. Duenow, D. Kuciauskas and A. B. J. Kanevce, "Comparison of Minority Carrier Lifetime Measurements in Superstrate and Substrate CdTe PV Devices," in *37th IEEE Photovoltaic Specialists Conference*, Seattle, Washington, 2011.

[26] I. Chang, "Chapter 6 Nonequilibrium Excess Carriers in Semicondutors," 11 09 2015. [Online]. Available: www2.ess.nthu.edu.tw/ikschang/letter/introduction%20to%20Solid-State%20Electronic%20Devices/Chapter%206.pdf.

[27] H. Myers, Introductory Solid State Physics, Bristol, Pennsylvania: Taylor & Francis, 1990, p. 83.

[28] J. Sites, "Characterization and Analysis of CIGS and CdTe Solar Cells," in *National Renewable Energy Laboratory*, Fort Collins, 2008.

[29] R. Triboulet and P. Siffert, CdTe and Related compounds; Physics, Defects, Hetero- and Nano-Sstructures, Crystal Growth, Surfaces and Applications, Oxford: Elsevier, 2010, pp. 54-56.

[30] Z. Cheng, A. E. Delahoy, Z. Su and K. K. Chin, "Steady state minority carrier lifetime and defect level occupation in thin film CdTe solar cells," *Thin Solid Films,* vol. 558, pp. 391-399, 2014 May 2.

[31] M. Fischetti, "ECE344 Semiconductor Devices and Materials (Fall 2009)," Fall 2009. [Online]. Available: http://www.ecs.umass.edu/ece/ece344/ECE344_2.pdf.

[32] C. Gianluca, N. Ettore, P. Vasantha and U. Nishad, "Effect of Bandgap Narrowing on Performance," *IEEE TRANSACTIONS ON ELECTRON DEVICES,* vol. 60, no. 12, pp. 4185-4190, dECEMBER 2013.

[33] I. Dharmadasa, "Review of the CdCl2 Treatment Used in CdS/CdTe Thin Film Solar Cell Development and New Evidence towards Improved Understanding," *Coatings,* vol. 4, pp. 282-307, 30 April 2014.

[34] M. Carmody, A. Gilmore and E. Technologies, "High Efficiency Single Crystal CdTe Solar Cells," National Renewable Energy Laboratory, Golden, 2011.

[35] B. Maniscalco, A. Abbas, J. Bowers, P. Kaminski, K. Bass, G. West and J. Walls, "The activation of thin film CdTe solar cells using alternative chlorine containing compounds," *Thin Solid Films,* vol. 582, pp. 115-119, 1 May 2015.

[36] I. The MathWorks, *MATLAB and Statistics Toolbox Release 2015,* Natick, Massachusetts, 2015.

Appendix A

Matlab - Main Program

```
function TRPL


% Constants:

%d = 3e-4; %thin film only: Absorber thickness, cm
d = 800e-4; % Single crystal thickness

dt = 16e-12; % Time step in IRF and measurement
tMax = 50e-9; % Maximum decay time to model

% Read and smooth IRF and Measurement
IRF = getIRF;
[tMeas, Meas] = SmoothingSample(getSAMPLE, tMax, dt);
tMax = max(tMeas);

% Initial guess:  Thin Film:
% Sf = 1e3; %Surface Recombination
% Sb = 1e6; %Bulk Recombination
% Mu = 50; %Mobility
% Tau = 2e-8; %Lifetime
% Bkg = 1e-2; %Background

%Initial Guess: Single Crystal:
Sf = 1e3; %Surface Recombination
Sb = 1e7; %Bulk Recombination :thermo velocity
Mu = 100; %Mobility
Tau = 2e-8; %Lifetime
Bkg = 1e-2; %Background

z0 = [Sf, Sb, Mu, Tau, Bkg]; % init guess

%Thin Film:
%zMin = [1e1, 1e6, 1, 1e-9, 5e-2]; % lower bounds
%zMax = [1e5, 1e6, 100, 1e-7, 1e-1]; % uppper bounds
```

```
%Single Crystal: with clean
zMin = [1e-1, Sb, 2, 1e-9, 5e-5]; % lower bounds
zMax = [1e5, Sb, 1000, 1e-5, 1e-1]; % uppper bounds 500 was the
mobility bound.


options = optimset('MaxFunEvals', 250, 'MaxIter', 300);


z = fminsearchbnd(@Error1, z0, zMin, zMax, options);

    function E = Error1(z)
        Fit = ConvModel( z, IRF, dt, tMax, tMeas, d) ;
        E = norm(1 - Fit./ Meas);
        sprintf('Error = %3.3f, Sf = %3.1e, Sb = %3.1e, Mu = %3.1f, Tau
= %3.1e, Bkg = % 3.1e', E, z)

    end

Fit = ConvModel( z, IRF, dt, tMax, tMeas, d) ;
semilogy(tMeas, Meas, tMeas,Fit);
grid on; hold on; drawnow;
title('SingleCrystalSample: W/HCL Dip: CdTeSideUp');
xlabel('Time(sec)');
ylabel('Counts(a.u)');
legend ('Sample', 'Fit');

end
```

Appendix B

Matlab - GetIRF

```
function IRF = getIRF
%this function returns new tIRF and IRF inside the desired iRange of
data
%that clips the noise from the real signal.
% used this is used in the main Thesis PDEPE Code for the thesis.
%%
ndata =
xlsread('C:\Users\FS100117\Documents\School\Thesis\Matlab\rewrite\IRF.x
lsx');

IRFCounts = ndata(1:6250,2);
IRF = IRFCounts; % Only select significant values
IRF = IRF / max(IRF); % Normalize the IRF data.
IRF = IRF(IRF > 1e-2);

% Smooth IRF:
tt = (0:(length(IRF)-1));
Window = 3;
ppY = SmartSmooth(tt, log(IRF), floor(length(IRF) / Window));
%smoothing is easy with log. window = average 3 pts. in series defines
the max freq allowed.


IRF = exp(fnval(ppY, tt));


end
```

Appendix C

Matlab - GetSample

```
function Sample = getSAMPLE(dt)
%this function returns new tSample and Sample inside the desired iRange
of data
%that clips the noise from the real signal.
% used this is used in the main Thesis PDEPE Code for the thesis.
%%
%[ndata, text, alldata] = xlsread('SampleA_ZNOSideUp_REPFREQ8.xlsx');
[ndata, text, alldata] = xlsread('SampleA_CdTeSideUp_REPFREQ8.xlsx');
%[ndata, text, alldata] = xlsread('SampleB_ZNOSideUp_REPFREQ8.xlsx');
%[ndata, text, alldata] = xlsread('SampleB_CdTeSideUp_REPFREQ8.xlsx');
%[ndata, text, alldata] = xlsread('SampleC_Sunnyside_ REPFREQ8.xlsx');
%[ndata, text, alldata] = xlsread('SampleC_Filmside_ REPFREQ8.xlsx');

Time = ndata(1:6250,1);

SampleCounts = ndata(1:6250,2);
%Time = (0:(length(SampleCounts)-1)) * dt;

%% Plots the Sample signal to verify it looks correct.
% figure
% semilogy(Time,SampleCounts,'g');xlabel('Time(ns)');ylabel('Sample-
Counts');grid on; hold on
% title('Sample Signal')
% xlabel('Time')
% ylabel('Counts')
%return

%%
iRange = find(SampleCounts>50); %gets rid of the noise in the data.
Sample = SampleCounts(iRange); % Sample counts inside the iRange
%tSample = Time(iRange); % Sample Time that corresponds to the Sample
counts inside the iRange.

% normalize the Sample data.
%max(Sample);
%Sample = Sample / max(Sample);
```

```
%return
%% this will plot the values but only for debugging purposes.
% figure
%
semilogy(Time(iRange),SampleCounts(iRange),'r');xlabel('Time(s)');ylabe
l('IRF-Counts');grid on; hold on
%  title('Clipped Sample')
%  xlabel('Time')
%  ylabel('Counts')

end
```

Appendix D

Matlab - SmoothingSample

```
function [tMeas, Meas] = SmoothingSample(Meas, tMax, dt)
%SmoothingSample Summary of this function goes here
%   takes in the clipped Sample and will smooth it out.

tt = (0:(length(Meas) - 1));
%semilogy(tt, Meas); grid on; hold on;
% Set filter window and run smoothing spline
Window = 7; % window at 40 works with other samples.
[ppMeas, Meas] = SmartSmooth(tt,Meas, floor(length(Meas) / Window));
%semilogy(tt, Meas); grid on; hold on;


[MMax, iMax] = max(Meas);
Meas = Meas(iMax:end) / MMax; %normalize data
tt = (0:length(Meas) - 1) * dt;


%semilogy(tt, Meas); grid on;
tSpreadingFactor = 1;
t = (0:29) .^ tSpreadingFactor;
tMeas = t / max(t) * max(tt);

Meas = csapi(tt, Meas, tMeas);

%semilogy(tMeas, Meas, '*'); grid on;

End
```

Appendix E

Matlab - Model

```
function  It = Model( z, d, tspan, nmesh )
%UNTITLED Summary of this function goes here
%   Detailed explanation goes here
% solves diff. eq. gives ideal curve.
% z = vector of the 4 parameters.
% d = absorber thickness
% tmax = total time of decay
% nmesh = n number of mesh points.
Sf = z(1);
Sb = z(2);
Mu = z(3);
Tau = z(4);

% thin film only
%xmesh = linspace ( 0.0, d, nmesh );

%Single Crystal
xmesh = SXMesh( d, nmesh );
% x = exp(0 : nmesh - 1) - 1;
% x = (0:nmesh-1) .^ 5;
% xmesh = x / max(x) * d;


%Constants:
Vt = 0.02585; %Thermal voltage, eV

%%
%u = time & space distrubution of e/h pairs.
u = pdepe ( 0, @pdefun, @icfun, @bcfun, xmesh, tspan );
It = zeros(size(tspan));
%
for i=1:length(tspan);
    It(i)= trapz(xmesh,u(i,:).^2); %intergrated value "It" = normalized
fit intergrated at each point. ideal TRPL fit
end
% don't care about band to band recombination rate constant because we
```

```
% normalize decays.
It = It / max(It);

    function [ c, f, s ] = pdefun(~,~,u,dudx)

        D = Mu * Vt;
        c = 1;
        f = dudx*D;
        s = (-u/Tau);

    end

%%
% % icfun: A handle to a function that defines the initial conditions
    function u = icfun(x) %does this c need to equal u0??

        Alpha = 1e6;

        u = exp(-Alpha*x);

     end
%%

    function [pl,ql,pr,qr] = bcfun(~,ul,~,ur, t)

        pl = Sf*ul;
        ql = -1;
        pr = Sb*ur;
        qr = 1;

    end

end
```

Appendix F

F Matlab - ConvModel

```
function Counts = ConvModel( z, IRF, dt, tMax, tMeas, d)
%takes the model and convolutes it with the IRF.
%ySplIRF : spline fit of the clipped IRF.
% t : time

%% Convolution:
tspan = 0: dt: tMax*1.2; % tpan starts steps stops.
nmesh = 20; %20 for HCL samples

M = Model( z, d, tspan, nmesh );
%semilogy(M); grid on; hold on;
%semilogy(IRF); grid on; hold on;
%conv2
Counts = conv(M, IRF, 'full'); % Convolute the Model curve with the
IRF.
%semilogy(Counts); grid on;
[CMax, iMax] = max(Counts);

Counts = Counts(iMax:end); %rescale
t = (0:(length(Counts) - 1)) * dt;
t = t( t < tMax);
Counts = Counts(1:length(t));
Counts = Counts / CMax; % Normalize the data
%semilogy(Counts); grid on;

Counts = csapi(t, Counts, tMeas) + z(5);

%semilogy(tMeas, Counts, '*'); grid on;

End
```